

Energy balance closure of eddy-covariance data: A multisite analysis for European FLUXNET stations

H.J. Hendricks Franssen^{a,b,c,*}, R. Stöckli^d, I. Lehner^a, E. Rotenberg^e, S.I. Seneviratne^a

^a Institute of Atmospheric and Climatic Sciences, ETH Zurich, 8092 Zurich, Switzerland

^b Institute of Environmental Engineering, ETH Zurich, 8093 Zurich, Switzerland

^c Agrosphere, ICG-4, Forschungszentrum Jülich GmbH, Leo Brandtstrasse, 52425 Jülich, Germany

^d Meteowiss, Climate Services, Climate Analysis, Krähbühlstrasse 58, 8044 Zurich, Switzerland

^e Department of Environmental Sciences and Energy Research (ESER), The Weizmann Institute of Sciences, Rehovot 76100, Israel

ARTICLE INFO

Article history:

Received 6 June 2009

Received in revised form 13 August 2010

Accepted 16 August 2010

Keywords:

Land–atmosphere interactions
Eddy covariance flux measurements
Energy balance closure
Atmospheric stability
Friction velocity
Thermal turbulence

ABSTRACT

This paper presents a multi-site (>20) analysis of the relative and absolute energy balance (EB) closure at European FLUXNET sites, as a function of the stability parameter ξ , the friction velocity u_* , thermally-induced turbulence, and the time of the day. A focus of the analysis is the magnitude of EB deficits for very unstable conditions. A univariate analysis of the relative EB deficit as function of ξ alone (both for individual sites and a synthesis for all sites), reveals that the relative EB deficit is larger for very unstable conditions ($\xi < -1.0$) than for less unstable conditions ($-0.02 > \xi \geq -1.0$). A bivariate analysis of the relative EB deficit as function of both ξ and u_* , however, indicates that for situations with comparable u_* the closure is better for very unstable conditions than for less unstable conditions. Our results suggest that the poorer closure for very unstable conditions identified from the univariate analysis is due to reduced u_* under these conditions. In addition, we identify that the conditions characterized by smallest relative EB deficits (elevated overall turbulence, mostly during day time) correspond to cases with the largest absolute EB deficits. Thus, the total EB deficit at the sites is induced mostly under these conditions, which is particularly relevant for evapotranspiration estimates. Further, situations with the largest relative EB deficits are generally characterized by small absolute EB deficits. We also find that the relative EB deficit does generally not correspond to the regression line of absolute EB deficit with the net radiation because there is a (positive or negative) offset. This can be understood from theoretical considerations. Finally, we find that storage effects explain a considerable fraction of the large *relative* (but small absolute) nocturnal EB deficits, and only a limited fraction of the overall relative and absolute EB deficits.

© 2010 Elsevier B.V. All rights reserved.

1. Introduction

Eddy-covariance (EC) flux measurements allow the assessment of land–atmosphere fluxes (e.g., carbon, water, and energy). They are now collected at several sites across the world as part of the FLUXNET network (e.g. Baldocchi et al., 2001). These data are essential for the estimation of the terrestrial water, energy and carbon balances, and for the understanding of the related physical and biological processes. This is of key relevance given the role of land surface processes for the climate system (e.g., Koster et al., 2004; Seneviratne et al., 2006; Friedlingstein et al., 2006). EC data are particularly useful for validating ecosystem, land-surface and climate

models (e.g., Baldocchi and Wilson, 2001; Stöckli et al., 2008; Jaeger et al., 2009).

However, EC data are subject to important random errors (e.g., Richardson et al., 2006, 2008), problems like footprint heterogeneity (i.e., the turbulent fluxes show a strong spatial variation around the measurement tower; e.g., Göckede et al., 2008; Vanderborght et al., 2010), incomplete time series because some of the measured turbulent fluxes are excluded when deemed unreliable (e.g., Falge et al., 2001; Schmid et al., 2003), and especially, the systematic error related to the energy balance (EB) closure problem (e.g., Twine et al., 2000; Finnigan et al., 2003; Meyers and Hollinger, 2004; Barr et al., 2006; Foken, 2008). This latter issue is the main focus of the present study.

Several hypotheses underlie the estimation of turbulent fluxes from EC data: (1) the ergodic hypothesis (i.e., the time average converges over an appropriate time interval to the ensemble average); (2) the Taylor hypothesis (i.e., the temporal average replaces the spatial average); (3) statistical stationarity for the period under

* Corresponding author at: Agrosphere, ICG-4, Forschungszentrum Jülich GmbH, Leo Brandtstrasse, 52425 Jülich, Germany. Tel.: +49 2461614462.

E-mail address: h.hendricks-franssen@fz-juelich.de (H.J.H. Franssen).

consideration (i.e., the mean flux should not change significantly over the averaging time used to determine the mean); (4) horizontal homogeneity; and (5) the assumption that the average vertical wind component is equal to zero. The vertical sensible and latent heat flux densities are evaluated by the EC method according to:

$$Q_H \equiv \rho c_p \overline{w'\theta'} \quad (1)$$

$$Q_E \equiv \rho l_v \overline{w'q'}, \quad (2)$$

where Q_H is the sensible heat flux density ($W m^{-2}$), Q_E the latent heat flux density ($W m^{-2}$), ρ the air density ($kg m^{-3}$), c_p the specific heat of moist air at constant pressure ($J kg^{-1} K^{-1}$), w the vertical wind velocity ($m s^{-1}$), θ the potential temperature (K), l_v the latent heat of vaporization ($J kg^{-1}$), and q the specific humidity (kg water vapor/kg air). An overbar denotes averaging over time and a prime denotes a fluctuation from the mean.

Eqs. (1) and (2) are often evaluated for high-resolution (e.g., 10 Hz or 20 Hz) EC data. In most cases, the energy flux densities estimated on the basis of EC data (the sum of sensible and latent heat flux densities) over 30-min periods, do not sum up to net radiation together with measured soil heat flux density and heat storage. The evaluation of EC data over longer time periods often leads to a better closure (e.g., Jarvis et al., 1997). For half-hourly values, Wilson et al. (2002) report an average EB deficit of 21% over 22 FLUXNET sites, and Barr et al. (2006) report for three mature boreal forest stands in Canada EB deficits between 11% and 15%.

The exact factors leading to EB deficits are still debated. Neglecting heat storage in soil and canopy, as well as measurement errors have been suggested to have a substantial impact on the EB closure. However, increasing measurement precision for net radiation and soil heat flux density makes it less likely that measurement errors in these components are the main causes of the energy balance deficit (e.g., Foken, 2008). Another explanation that has been put forward in recent years, is that the EB closure problem may be related to low frequency turbulence that is not included in Eqs. (1) and (2), principally because the period over which the averages are calculated is relatively short (e.g., Finnigan et al., 2003; Foken et al., 2006). Indeed, coherent structures that are “attached” to the landscape may develop and these are not sampled with the EC method (e.g., Inagaki et al., 2006). This may be induced by e.g. land surface heterogeneities generating eddies at larger scales than those captured by the standard application of the EC method (e.g. Kanda et al., 2004; Inagaki et al., 2006; Mauder et al., 2007; Huang et al., 2009).

Previous studies based on experimental data suggested that the relative EB closure improves for increasing friction velocities u_* and increasing instability (e.g., Wilson et al., 2002; Barr et al., 2006). Under unstable conditions, convection is not suppressed and many studies find that the EC technique results in smaller relative EB deficits (e.g., Wilson et al., 2002; Barr et al., 2006). Also large u_* reduces the relative EB closure problem (e.g., Wilson et al., 2002; Barr et al., 2006), because the ergodic hypothesis and Taylor hypothesis are better fulfilled. However, under very unstable conditions also more low frequency turbulence (i.e., larger eddies) may be generated, for instance due to the occurrence of organized convection, meso-scale circulation systems or the development of deeper boundary layers (e.g., Finnigan et al., 2003). As mentioned, this may lead to a worsening of the EB closure for these conditions.

Indeed, from Figs. 4 and 5 in Barr et al. (2006) it can be seen that the relative EB closure is poorer for very unstable conditions than for less unstable conditions, although this result is not discussed in detail. Also Tanaka et al. (2008) find a larger relative EB deficit for very unstable conditions. Finnigan et al. (2003) hypothesize that a poorer relative EB closure induced by low frequency turbulence (related with large-scale convection), is expected to affect forested sites (high sensors) more than agricultural lands (low sensors).

In order to derive firmer conclusions concerning the EB closure under very unstable conditions, it is necessary to expand these results with a multi-site analysis. In the present study, we investigate EC data from up to 26 European FLUXNET sites, with a focus on the following questions:

- (1) Is the larger relative EB deficit reported in the literature for very unstable conditions (compared with less unstable conditions) robust when analysed for a large number of sites?
- (2) What are the relative contributions of mechanically- vs. thermally-induced turbulence for relative EB deficits under very unstable conditions?
- (3) Does a multi-site analysis of the relative EB deficit as function of three or four variables (atmospheric stability ξ , u_* , thermal turbulence, time of the day) provide new insights regarding the relation between relative EB deficit and environmental factors?
- (4) How does the *absolute* EB deficit relate with the *relative* EB deficit under different atmospheric conditions?
- (5) How can cases with particularly poor EB closure be interpreted? Are such cases concomitant with conditions of small absolute net radiation?

Details on data and methods are provided in the next section, the results and analyses are presented in Section 3, and the main conclusions of this study are highlighted in Section 4.

2. Data and methods

2.1. Data

Flux tower data from 26 European FLUXNET sites, of which 21 forested sites, are analyzed here for the years 1997–2006 (Table 1). For some analyses the total number of considered sites is smaller when data was unavailable for given variables (e.g. no ξ data at Flakaliden and no u_* data at Bayreuth and Flakaliden, and missing storage data at many of the sites). The time series at the considered sites include at least two years with net radiation, turbulent flux densities and soil heat flux density. The turbulent fluxes for the European FLUXNET sites are estimated on the basis of 30-min averages. Table 1 provides more information about the sites. For further details, we refer the reader to the respective publications and references therein, or to the official FLUXNET homepage (<http://www.fluxnet.ornl.gov>).

The data were extracted from the common database and underwent a pre-screening. For this study, additional checks were made and for some sites erroneous radiation measurements were eliminated from the analysis. If for a given 30-min period net radiation, latent and sensible heat flux densities, soil heat flux density and storage terms are available, the energy balance deficit can be expressed as follows:

$$\Delta EB = R_n - Q_H - Q_E - Q_G - \Delta S_{LE} - \Delta S_H - \Delta S_{BIO} - \Delta S_G, \quad (3)$$

where ΔEB is the absolute EB deficit ($W m^{-2}$), R_n the net radiation ($W m^{-2}$), Q_G the soil heat flux density ($W m^{-2}$), and ΔS energy storage ($W m^{-2}$) as latent heat between the soil surface and the EC sensors (hereinafter: in the canopy air space) (ΔS_{LE}), as sensible heat in the canopy air space (ΔS_H), in the biomass (ΔS_{BIO}) and in the soil layer between the heat flux plate and the soil surface (ΔS_G). The relative EB deficit is the absolute EB deficit standardized by R_n . In Section 2.2 details are provided on the calculation of the relative EB deficit.

In this study the energy storage terms are generally not considered in the analysis, because these data are only available for a limited number of sites, and in case of ΔS_G for none of the sites. However, the contribution of heat storage to the half-hourly energy

Table 1

Details about the 26 European FLUXNET sites used in this study. UK: United Kingdom. Vegetation types: BET: evergreen broad leaf, BDT: deciduous broad leaf, MF: mixed forest, NET: evergreen needle leaf, Crop: crops or grassland.

Site and country	Longitude (°)	Latitude (°)	Altitude (m.a.s.l.)	Sensor height (m)	Vegetation type	No. of years	Site reference
Amplero (Italy)	13.605 E	41.904 N	884	4	Crop	4	Gilmanov et al. (2007)
Bayreuth (Germany)	11.868 E	50.142 N	780	32	NET	3	Staudt and Foken (2007)
Brasschaat (Belgium)	4.521 E	51.309 N	16	42	MF	2	Gielen et al. (2010)
Castel-Porziano (Italy)	12.378 E	41.706 N	68	25	BET	8	Reichstein et al. (2002)
Collelongo (Italy)	13.589 E	41.849 N	1550	32	BDT	8	Valentini et al. (2000)
East-Saltoun (UK)	−2.500 W	55.900 N	97	3	Crop	2	www.fluxdata.org
El Saler (Spain)	−0.519 W	39.346 N	10	15.5	NET	8	Reichstein et al. (2005)
Flakaliden (Sweden)	19.457 E	64.113 N	315	15	NET	7	Valentini et al. (2000)
Fyodorovskye (Russia)	32.924 E	56.462 N	265	29	NET	8	Milyukova et al. (2002)
Griffin (UK)	−3.797 W	56.607 N	340	15.5	NET	7	Valentini et al. (2000)
Grignon (France)	1.952 E	48.844 N	125	4	Crop	2	Hibbard et al. (2005)
Hainich (Germany)	10.452 E	51.079 N	430	44	BDT	4	Kutsch et al. (2010)
Hampshire (UK)	−0.861 W	51.121 N	80	28	BDT	2	www.fluxdata.org
Lonzee (Belgium)	4.745 E	50.552 N	165	2.7	Crop	2	Moureaux et al. (2006)
Loobos (Netherlands)	5.744 E	52.168 N	25	27	NET	7	Dolman et al. (2002)
Mehrstedt (Germany)	10.655 E	51.275 N	286	3	Crop	2	Don et al. (2009)
Nonantola (Italy)	11.089 E	44.690 N	25	15	BDT	3	Reichstein et al. (2003)
Renon (Italy)	11.435 E	46.588 N	1730	32	NET	2	Marcolla et al. (2003)
Roccarespampani (Italy)	11.930 E	42.408 N	234	18.5	BDT	4	Reichstein et al. (2003)
San Rossoro (Italy)	10.287 E	43.730 N	4	24	NET	6	Reichstein et al. (2005)
Sodankylä (Finland)	26.638 E	67.362 N	180	23.5	NET	6	Hatakka et al. (2003)
Tharandt (Germany)	13.567 E	50.964 N	380	42	NET	7	Grünwald et al. (2007)
Vielsalm (Belgium)	5.999 E	50.309 N	450	40	MF	9	Aubinet et al. (2001)
Wetzstein (Germany)	11.458 E	50.454 N	785	30	NET	3	Rebmann et al. (2010)
Yatir Forest (Israel)	35.052 E	31.345 N	650	18.7	NET	4	Grunzweig et al. (2003)
Zerbolo (Italy)	9.061 E	45.201 N	60	27.5	BDT	4	Migliavacca et al. (2009)

balance deficit is not negligible for tall vegetation (e.g., Foken et al., 2006) and also ΔS_C might play a role (e.g., Heusinkveld et al., 2004). Therefore for some of the sites, for which storage data are available, additional analyses are provided (Section 3.10). Not enough sites with storage terms were available to perform bi- and trivariate analyses, but the effect of storage is estimated for the individual sites with data, and as a multi-site analysis as function of ξ and time of the day. In order to further analyze the impact of excluding heat storage from Eq. (3) for a larger number of sites, ΔEB is also evaluated as a function of the time of the day. Indeed it is expected that during the morning energy storage is in most cases positive (resulting in a larger relative EB deficit), while during the afternoon the energy storage is in most cases not positive and very small. This analysis hence provides an indirect means to determine the role of energy storage for the relative EB closure, by identifying whether the relation between the atmospheric stability, thermal turbulence, u^* and relative EB closure, is different for conditions with positive energy storage (morning) and zero or negative energy storage (afternoons).

Our main focus is not on the magnitude of the relative EB deficits, but on their relation with the ξ , u^* , thermally-induced turbulence, and time of the day. Thus in this analysis, we also do not consider differences between open-path and closed-path EC measurements, though these may slightly impact relative EB deficits (with slightly larger relative EB deficits for the closed-path system, e.g. Wilson et al., 2002 and Haslwanter et al., 2009).

2.2. Method

The absolute and relative EB deficits, together with the average net radiation, are analysed for different subsets of the measured data:

(1) As a function of atmospheric stability, both for individual sites and as a multi-site analysis. EB closure is analyzed as a function of ξ for the individual sites, dividing the data points into four stability classes: stable ($\xi \geq 0.1$), neutral ($-0.1 < \xi < 0.1$), slightly

unstable ($-0.5 \leq \xi \leq -0.1$), and (very) unstable ($\xi < -0.5$). The classes are chosen such that each class has enough data points to provide a reliable estimate of the EB deficit. The ξ is also included in the European FLUXNET data set and is calculated as:

$$\xi = \frac{z-d}{L} \quad (4)$$

with:

$$L = \frac{-u_*^3}{k(g/\theta)w\theta'} \quad (5)$$

where z is the sensor height (m), d the zero-plane displacement height (m), L the Monin-Obukhov length (m), k the von Kármán constant ($-$), g the gravitational acceleration ($m s^{-2}$), and u^* the friction velocity ($m s^{-1}$). The analysis is repeated as a multi-site analysis, which is carried out for the 20 forested sites with a sensor height of at least 15 m. For this multi-site analysis the EB deficit is estimated for 19 different ξ classes.

For six sites (Vielsalm, Tharandt, Brasschaat, Castel Porziano, Loobos and Collelongo), results including ΔS_H and ΔS_{LE} are compared with results excluding storage, and for two sites (Vielsalm, Tharandt) also an analysis is made including ΔS_{BIO} . Brasschaat also recorded ΔS_{BIO} , but very infrequently, and is therefore excluded from the analysis.

- (2) As a function of u^* , as a multi-site analysis. For u^* a multi-site analysis is performed including all 24 sites with u^* data. In that case, the EB deficit is estimated as a function of u^* for 19 classes.
- (3) As a function of thermally-induced turbulence, as a multi-site analysis. Eq. (5) shows that ξ is impacted by u^* (numerator) and thermally-induced turbulence (TT, denominator). Here we address the following question: is the relative EB deficit under very unstable conditions caused by reduced u^* , or by elevated TT generating more low frequent turbulence (not captured by the standard integration time used at the European FLUXNET sites)?
- (4) As a function of the time of the day, as a multi-site analysis. In this case the EB deficit is estimated on an hourly basis. The times

Table 2
Average EB deficits (%) for 25 European FLUXNET sites and four ξ classes. In brackets the number of data points is given. The grey shading indicates which class has the lowest to the highest (light to dark grey) relative EB deficit.

Site	$\xi < -0.5$	$-0.5 \leq \xi \leq -0.1$	$0.1 > \xi > -0.1$	$\xi \geq 0.1$	All data
Tall vegetation					
Bayreuth	24.6 (n = 876)	22.7 (n = 1896)	46.3 (n = 8909)	68.4 (n = 1859)	28.9
Brasschaat	28.7 (n = 1019)	22.8 (n = 1450)	45.5 (n = 6255)	89.8 (n = 1071)	34.1
Castel-Porziano	29.7 (n = 3781)	20.9 (n = 9284)	23.8 (n = 25499)	60.4 (n = 15575)	26.4
Collalongo	34.8 (n = 4326)	29.7 (n = 2728)	39.8 (n = 6621)	15.0 (n = 5781)	29.0
El Saler	25.4 (n = 1033)	14.9 (n = 3174)	17.5 (n = 9117)	62.9 (n = 2633)	17.8
Fyodorovskye	30.7 (n = 1575)	26.2 (n = 4996)	24.6 (n = 40015)	79.5 (n = 6119)	26.8
Griffin	15.5 (n = 1812)	9.0 (n = 2199)	9.4 (n = 16910)	73.3 (n = 3986)	11.1
Hainich	30.7 (n = 1858)	23.6 (n = 3459)	24.3 (n = 20594)	71.3 (n = 4330)	26.6
Hampshire	51.1 (n = 626)	26.6 (n = 633)	35.8 (n = 9569)	68.1 (n = 1454)	35.0
Loobos	18.3 (n = 2290)	15.6 (n = 4633)	19.3 (n = 21373)	63.9 (n = 8411)	16.9
Nonantola	32.1 (n = 2592)	34.3 (n = 1846)	54.9 (n = 4489)	78.7 (n = 5426)	38.3
Renon	Few data	Few data	-4.5 (n = 7113)	7.4 (n = 721)	11.1
Roccarespanpani	31.5 (n = 1602)	24.6 (n = 2406)	19.0 (n = 15073)	88.3 (n = 4781)	23.3
San Rossoro	39.6 (n = 1656)	32.7 (n = 5314)	36.0 (n = 15804)	71.5 (n = 8178)	34.5
Sodankyla	25.3 (n = 2348)	19.2 (n = 3913)	23.8 (n = 22916)	73.8 (n = 5855)	25.5
Tharandt	20.1 (n = 2856)	17.5 (n = 5992)	17.0 (n = 30902)	68.4 (n = 8668)	18.9
Vielsalm	34.7 (n = 4577)	27.0 (n = 6422)	39.8 (n = 24031)	58.6 (n = 9513)	30.2
Wetzstein	33.0 (n = 735)	28.8 (n = 2005)	39.8 (n = 11724)	67.8 (n = 1396)	33.6
Yatir Forest	28.9 (n = 764)	13.0 (n = 1888)	8.9 (n = 4339)	80.2 (n = 2117)	14.3
Zerbolo	35.6 (n = 2283)	30.3 (n = 2313)	37.8 (n = 6668)	61.9 (n = 4766)	34.8
Short vegetation					
Amplero	16.1 (n = 5534)	12.4 (n = 3347)	30.6 (n = 8152)	60.4 (n = 3666)	17.3
East-Saltoun	51.8 (n = 464)	50.4 (n = 764)	51.4 (n = 6803)	96.0 (n = 902)	51.3
Grignon	33.7 (n = 165)	31.2 (n = 696)	31.9 (n = 6409)	80.3 (n = 566)	32.0
Lonzee	8.0 (n = 195)	7.3 (n = 994)	6.1 (n = 8485)	-18.2 (n = 1655)	5.9
Mehrstedt	23.0 (n = 1262)	16.2 (n = 1986)	20.8 (n = 13060)	68.1 (n = 3479)	21.5
Average tall vegetation (without Renon)	30.0	23.1	29.6	68.5	25.9
Average short vegetation	26.5	23.5	28.2	57.3	25.6
Average over 25 sites	29.3	23.2	28.0	63.8	25.8

are local times. This analysis was also carried out including the role of storage, using the six sites mentioned under 1).

(5) As a joint function of two of the four above-mentioned variables, namely:

- u_* and ξ or TT.
- ξ and time of the day.
- TT and time of the day.
- u_* and time of the day.

For these analyses the following five different ξ classes were considered: very unstable ($\xi \leq -1.0$), unstable ($-0.02 \geq \xi > -1.0$), neutral ($0.02 > \xi > -0.02$), stable ($1.0 > \xi \geq 0.02$), and very stable ($\xi \geq 1.0$). Analyses were made for four different local time periods (0–6 h, 6–12 h, 12–18 h, and 18–24 h), five different TT classes ($TT < -3 \times 10^{-4} \text{ m}^2 \text{ s}^{-3}$, $-3 \times 10^{-4} \text{ m}^2 \text{ s}^{-3} \leq TT < -1 \times 10^{-4} \text{ m}^2 \text{ s}^{-3}$, $-1 \times 10^{-4} \text{ m}^2 \text{ s}^{-3} \leq TT < 1 \times 10^{-4} \text{ m}^2 \text{ s}^{-3}$, $1 \times 10^{-4} \text{ m}^2 \text{ s}^{-3} \leq TT < 1 \times 10^{-3} \text{ m}^2 \text{ s}^{-3}$, $TT \geq 1 \times 10^{-3} \text{ m}^2 \text{ s}^{-3}$), and five different u_* classes ($u_* < 0.15 \text{ m s}^{-1}$, $0.15 \leq u_* < 0.30 \text{ m s}^{-1}$, $0.30 \leq u_* < 0.45 \text{ m s}^{-1}$, $0.45 \leq u_* < 0.60 \text{ m s}^{-1}$, and $u_* \geq 0.60 \text{ m s}^{-1}$).

(6) As a joint function of all variables: u_* , ξ (or TT) and time of the day. In this case the analysis was made for five ξ classes (similar to 5a and b) or five different classes for TT (similar to 5a and c), five u_* classes (similar to 5a and d), and four different local time periods (similar to 5b–d).

For each of the individual cases that comprise the different analyzed subsets, the overall relative EB deficit is determined by the weighted least squares regression of its single values as a function of net radiation with zero offset. The regression slope gives the relative EB deficit as a fraction, expressed in %. This procedure is commonly used to estimate the relative EB deficit (e.g., Wilson et al., 2002; Barr et al., 2006) and was justified (e.g., Wilson et al.,

2002) by the fact that the differences between regression with and without offset are in most cases small (see however later discussions, Section 3.2 and Table 3). The 95% estimation interval of the regression slope (the regression coefficient) is also determined.

Also a weighted least squares regression is performed allowing the offset being different from zero. We argue that for non-neutral atmospheric conditions it is necessary to allow for an offset in the regression. During unstable conditions or positive TT, the offset is expected to be negative, whereas it is expected to be positive for stable conditions or negative TT. We find that this is indeed the case (see later discussion, Section 3.2 and Table 3). The reason why offsets are expected to be different from zero can be understood better if one has a closer look at the denominator of Eq. (5). Let us consider the case that a regression is made of the EB deficit as a function of net radiation, for a subset of measured data with $TT > 0$. Evidently, $TT \gg 0$ is associated with a strong positive sensible heat flux density, and if this observation is associated with a measured net radiation equal to zero, it is expected that the EB deficit is negative and this results in a negative offset. In theory, the energy balance still could be close to zero if the soil heat flux density would be strongly negative, which is not common under these conditions. The opposite is the case for $TT < 0$. In this case the offset is expected to be positive. The same problem affects regressions considering subsets of measured data with different observed atmospheric stability. In case of an unstable atmosphere ($\xi < 0$), the offset is expected to be negative, and for a stable atmosphere ($\xi > 0$) it is expected to be positive. Also for subsets of the measured data with different u_* values, the offset cannot be expected to be zero, given the correlation between u_* and the atmospheric stability parameter.

Finally, the relative EB deficit was also estimated by the bulk method with the following formula: $\sum(Q_H + Q_E) / \sum(R_n - Q_G)$. All fluxes are summed up over all measurements over given subsets of the data. However, because this method in general did not provide

reliable results, few results from the bulk method will be presented in this paper.

For the analysis of the absolute EB deficits, one should take into account that the deficits are affected by systematic errors (e.g. density effects and sensor separation for measurements of the latent heat flux density). Additionally, neglecting storage might affect the absolute EB deficits, especially if they are analyzed for transitional time periods at sunrise or sunset, or certain specific atmospheric conditions (particularly stable nighttime situations). The impact of storage is analyzed in detail for the mentioned subset of sites. As a result, we assume that absolute EB deficits of up to 20 W m^{-2} can be attributed to systematic measurement errors and/or neglected storage terms, and not to any atmospheric mechanisms/processes forcing an EB deficit.

3. Results and discussion

3.1. EB closure as a function of ξ at individual sites

Table 2 displays the relative EB deficits for the individual sites, for different ξ classes. For most sites (23 out of 24) the relative EB deficit is larger for (very) unstable conditions ($\xi < -0.5$) than for slightly unstable conditions ($-0.5 \leq \xi \leq -0.1$). For Renon (Italy) not enough data for unstable conditions are available to make a reliable estimate of the EB deficit. Averaged over all sites, the EB deficit for $\xi < -0.5$ is 29.3% whereas it is 23.2% for $-0.5 \leq \xi \leq -0.1$. The 19 sites with tall vegetation have an average relative EB deficit that is 6.9 percent points (± 1.3) larger for $\xi < -0.5$ than for $-0.5 \leq \xi \leq -0.1$, whereas for the five sites with short vegetation the difference is 3.0 percent points (± 1.1) only. The differences are significant ($p < 0.05$). Also remarkable is the bad closure for stable conditions ($\xi \geq 0.1$) with EB deficits between 60% and 90% for most of the sites.

Taking into account all ξ classes, the impression may arise from Table 2 that the relative EB deficit is much larger than reported in other studies for FLUXNET studies (e.g., Wilson et al., 2002). However, this is not the case. If all the data for a specific site are taken together, and a regression is performed to estimate the relative EB deficit for each site, the average relative EB deficit over all sites is 25.8% (see last column of Table 2), which is only marginally larger than the value reported by Wilson et al. (2002). The relative EB deficit is slightly larger because energy storage is not taken into account in the values provided in Table 2. Moreover, in this study a larger number of observations are included compared with Wilson et al. (2002), which might also impact the results. The relative EB closure was also alternatively determined for each site by the bulk method, where the quantities are determined over the complete time series. Over long time series the net change in storage is negligible compared to the total sum of net radiation and the total sum of the energy flux densities. Averaged over 25 sites the relative EB deficit is 23.4% with this method, which is only marginally smaller than the value found by the regression analysis (25.8%). Moreover, this method seems to give less reliable results because of the occurrence of outliers for two sites: a strongly negative relative EB deficit and an extremely large relative EB deficit, both values strongly deviating from the relative EB deficit estimated by regression.

The fact that the overall relative EB deficit is much lower than the averages over the different ξ classes can be explained by two main factors. First, there are often more measurements for the ξ classes that are associated with a smaller relative EB deficit. Second, if a regression is performed taking into account all data, the slope of the regression line is strongly determined by the EB deficit for the cases with an elevated net radiation. These cases occur during daytime and mostly under conditions where the EC technique performs well.

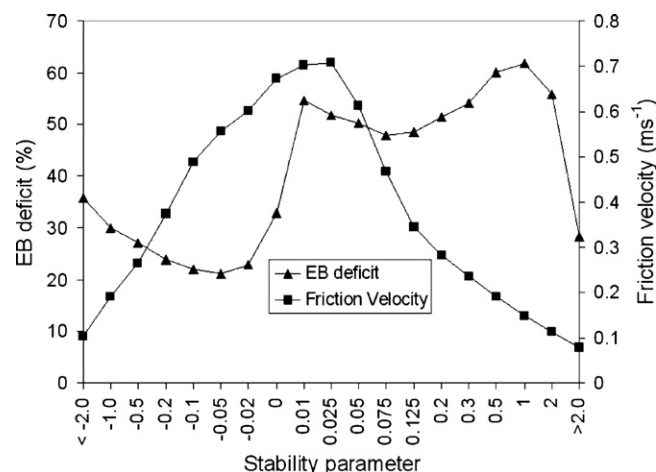


Fig. 1. The EB deficit and u_* as a function of ξ , on the basis of a multi-site-analysis over 20 European FLUXNET sites (tall vegetation only) with 486,462 data points in total and between 8,825 and 35,506 data points per ξ class (only four classes have less than 20,000 data). The upper boundary of the ξ class is given, the lower boundary value is given by the preceding value (for instance: -0.5 stands for the class with stabilities between -1.0 and -0.5). The uncertainty of the estimated EB deficit is very small (not shown).

3.2. Multi-site analysis of EB closure as a function of ξ

Here we perform a multi-site analysis in order to shed more light on the relation of the relative EB deficit with ξ . Fig. 1 shows clearly that for very unstable conditions the relative EB deficit is larger than for less unstable conditions. The EB deficit reaches a minimum of 21.2% for $-0.05 > \xi \geq -0.1$. For very unstable conditions with $\xi < -1.0$ the EB deficit is above 30%, for $\xi < -2.0$ even 35.7%. This illustrates that the increase of the relative EB deficit for very unstable conditions, already observed for the individual sites, is even more pronounced if we divide the data in a larger number of ξ classes, and have enough data to calculate the EB deficit for conditions that are very unstable. However, Fig. 1 also illustrates that the very unstable conditions are associated with much lower u_* than (slightly) unstable conditions. Lower u_* are in general associated with larger relative EB deficits. Therefore, from this analysis it remains unclear whether the increase of the relative EB deficit for very unstable conditions is related to issues induced by increased large values of TT, or to the reduced u_* . Fig. 1 also illustrates that around neutral conditions a very sudden change in the relative EB deficit occurs, with an EB deficit above 50% for close to neutral, very slightly stable conditions ($0.0 \leq \xi < 0.01$), and decreasing to 33% for close to neutral, very slightly unstable conditions ($-0.02 \leq \xi < 0.0$). The largest relative EB deficits are found for more stable conditions, with EB deficits larger than 60% for $0.3 \leq \xi < 2.0$. Surprisingly, for very stable conditions ($\xi \geq 2.0$) the relative EB deficit is much smaller than for less stable conditions. This is partly explained by the fact that a large part of the cases with very stable conditions can be attributed to the site of Collelongo, which has a very good EB closure for stable conditions in general.

For each ξ class, we performed a regression analysis of the EB deficit as a function of net radiation. The results are summarized in Table 3. Accounting for an offset results in negative offsets for unstable conditions and positive offsets for stable conditions. The offsets deviate by up to 22 W m^{-2} from the origin. These offsets also impact the slope of the regression equation, but do not modify the general findings highlighted earlier in this section. The results also indicate that close to neutral and unstable conditions are associated with a positive net radiation (above 300 W m^{-2} for $-0.1 > \xi \geq -0.5$), whereas stable conditions coincide with a slightly negative net radiation. The absolute EB deficit is therefore also larger for unstable

Table 3
Results for the multi-site analysis of the EB deficit as function of ξ . Presented are the results from the regressions of EB deficit as a function of net radiation (with and without offset) and also the average net radiation, the absolute EB deficit and the number of data points per ξ class. The uncertainty of the estimated EB deficit is very small (not shown).

ξ	EB deficit (%)	Offset (W m^{-2})	Slope for regression with offset $\times 100$ (%)	Average net radiation (W m^{-2})	Average EB deficit (W m^{-2})	Number of data points
$\xi < -2.0$	35.7	-10.9	38.0	110.8	31.2	13120
$-2.0 < \xi \leq -1.0$	30.0	-14.1	33.2	209.3	55.4	8825
$-1.0 < \xi \leq -0.5$	27.0	-15.4	30.4	270.3	66.8	13906
$-0.5 < \xi \leq -0.2$	23.8	-16.2	27.4	311.6	69.0	31562
$-0.2 < \xi \leq -0.1$	21.9	-18.4	25.9	318.6	64.2	33444
$-0.1 < \xi \leq -0.05$	21.2	-20.9	26.4	261.1	48.0	31289
$-0.05 < \xi \leq -0.02$	22.9	-19.9	28.4	187.6	34.3	29507
$-0.02 < \xi \leq 0$	32.8	-16.8	39.8	89.7	18.9	31519
$0 < \xi \leq 0.01$	54.6	9.4	50.8	21.0	20.1	31409
$0.01 < \xi \leq 0.025$	51.7	21.0	50.3	2.1	22.1	34511
$0.025 < \xi \leq 0.05$	50.3	21.9	55.8	-7.2	17.8	35506
$0.05 < \xi \leq 0.075$	47.8	21.4	60.0	-15.3	12.2	20540
$0.075 < \xi \leq 0.125$	48.6	20.3	63.8	-20.6	7.1	27558
$0.125 < \xi \leq 0.2$	51.4	17.9	69.0	-27.2	-0.9	25035
$0.2 < \xi \leq 0.3$	54.2	15.4	71.4	-31.8	-7.3	21214
$0.3 < \xi \leq 0.5$	60.2	12.6	75.4	-34.3	-13.3	25458
$0.5 < \xi \leq 1.0$	61.8	5.0	67.8	-34.7	-18.5	27595
$1.0 < \xi \leq 2.0$	55.8	-4.5	51.9	-32.6	-21.4	19403
$\xi > 2.0$	28.2	-17.1	25.8	-15.0	-20.9	25061

conditions, with deficits reaching almost 70 W m^{-2} for moderately unstable conditions ($-0.1 > \xi > -1.0$). This means that the EB deficit during daytime, under conditions when the EC method works well and with a rather low relative EB deficit, is of much more concern, e.g. for daily evapotranspiration estimates and the overall energy balance, than the EB deficit during stable conditions with large relative, but (very) small absolute values.

3.3. Multi-site analysis of EB closure as a function of u_*

Next, an overall assessment of the relation between u_* and the relative EB deficit is made on the basis of a multi-site analysis (Fig. 2). Clearly, the relative EB deficit is largest for very low u_* , and decreases continuously with increasing u_* . Here, the results are less affected by including an offset in the regression analysis. The fitted offsets are in all cases smaller than 10 W m^{-2} and have no significant effects on the fitted slope of the regression line. Fig. 2 shows

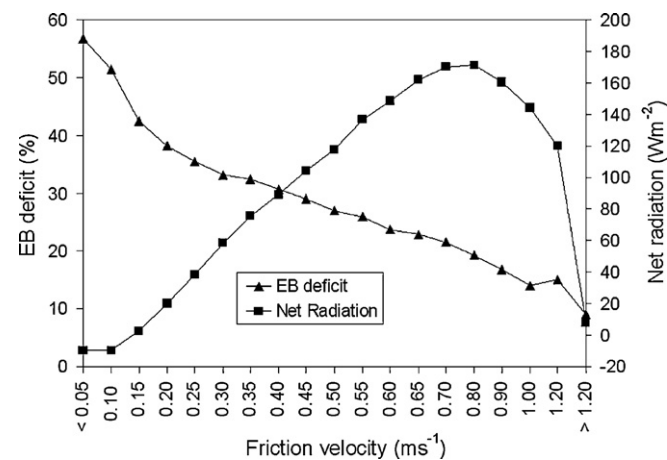


Fig. 2. The EB deficit and net radiation as a function of u_* , on the basis of a multi-site analysis over 24 European FLUXNET sites with 499,993 data points in total and between 11,830 and 41,845 data points per u_* -class with the exception of the class with $u_* > 1.2 \text{ m s}^{-1}$ (6396 observations only). The upper boundary of the u_* class is given, the lower boundary value is given by the preceding value (for instance: 0.30 m s^{-1} stand for the class with stabilities between 0.25 m s^{-1} and 0.30 m s^{-1}). The uncertainty of the estimated EB deficit is very small (not shown).

also the average net radiation as a function of u_* . More elevated u_* are associated with higher average net radiation. The net radiation is averaged over all cases, including all seasons of the year and all 24 flux towers.

3.4. Multi-site analysis of EB closure as a function of TT

The 17 classes for which the EB closure was calculated were defined such that the different classes had enough data points. The relative EB deficits as determined from the regressions without offset indicate an improved relative EB closure for increased TT (Table 4). The hypothesis that for very large TT the relative EB closure could be poorer than for less elevated TT does not seem to be valid. We find that for a regression with offset, the offset under conditions of a positive TT is negative, whereas the offset is larger than zero for $\text{TT} < 0$. The offsets are clearly larger than those for the regressions for (very) unstable conditions, and can even drop below -50 W m^{-2} for elevated positive values of TT. The relative EB deficit was also determined by the bulk method. However, this method gave reasonable results for unstable conditions only. For those classes where the number of data points with net radiation close to zero is large, as is the case for negative TT values, the bulk method does not provide reasonable results. For classes with an elevated positive TT, the bulk method gives a smaller relative EB deficit than estimated from the regression without offset. For TT values between $5 \times 10^{-4} \text{ m}^2 \text{ s}^{-3}$ and $1 \times 10^{-3} \text{ m}^2 \text{ s}^{-3}$ the deficit estimated with the bulk method is for example 26.8% compared to 33.6% for the regression-based method. Therefore, although the determination of the exact relative EB deficit is ambiguous, the data clearly indicate that the relative EB closure continues to improve for increased TT (although the size of the absolute EB deficit actually increases with increased TT, with the exception of the highest TT class).

If we analyze the results in terms of absolute EB deficits, the largest EB deficits are found for elevated positive TT values. TT values close to zero are associated with very small absolute EB deficits (2 W m^{-2} only) and also for stable conditions (with the exception of strongly negative TT values), the EB deficits are smaller than 20 W m^{-2} . Despite the fact that the largest relative EB deficits are found for negative TT values, for stable conditions the deficits are probably not significant, because for all except two classes the

Table 4

Results for the multi-site analysis of the EB deficit as function of TT (denominator of Eq. (5)). Presented are the results from the regressions of EB deficit as a function of net radiation (with and without offset) and also the average net radiation, the absolute EB deficit and the number of data points per class. The uncertainty of the estimated EB deficit is (very) small (not given).

$k(g/\theta)w\theta'(m^2s^{-3})$	EB deficit (%)	Offset ($W m^{-2}$)	Slope for regression with offset $\times 100$ (%)	Average net radiation ($W m^{-2}$)	Average EB deficit ($W m^{-2}$)	Number of data points
$TT > 4 \times 10^{-3}$	5.7	-63.4	16.3	494.8	17.1	6622
$2 \times 10^{-3} < TT \leq 4 \times 10^{-3}$	19.3	-141.5	46.1	459.4	70.5	27146
$1 \times 10^{-3} < TT \leq 2 \times 10^{-3}$	27.0	-97.5	50.2	341.6	73.9	39575
$5 \times 10^{-4} < TT \leq 1 \times 10^{-3}$	33.6	-56.3	52.1	217.9	57.4	33375
$1 \times 10^{-4} < TT \leq 5 \times 10^{-4}$	44.3	-21.4	53.6	111.7	38.3	50703
$1 \times 10^{-5} < TT \leq 1 \times 10^{-4}$	56.1	-5.8	58.4	32.0	12.9	29376
$0 < TT \leq 1 \times 10^{-5}$	60.0	-5.2	60.0	-0.3	-5.3	8691
$TT = 0$	44.7	-10.4	47.2	26.3	2.0	9623
$-1 \times 10^{-5} < TT < 0$	44.1	-10.6	41.4	-12.3	-15.7	14374
$-5 \times 10^{-5} < TT \leq -1 \times 10^{-5}$	57.7	3.0	57.0	-8.4	-7.7	39404
$-1 \times 10^{-4} < TT \leq -5 \times 10^{-5}$	60.4	1.2	60.8	-10.5	-5.2	40165
$-2 \times 10^{-4} < TT \leq -1 \times 10^{-4}$	61.3	7.4	65.3	-15.3	-2.7	60013
$-3 \times 10^{-4} < TT \leq -2 \times 10^{-4}$	51.7	12.6	60.0	-21.3	0.0	40399
$-5 \times 10^{-4} < TT \leq -3 \times 10^{-4}$	71.6	31.2	77.7	-27.6	4.5	45668
$-1 \times 10^{-3} < TT \leq -5 \times 10^{-4}$	30.3	32.2	54.5	0.6	-29.9	33986
$-2 \times 10^{-3} < TT \leq -1 \times 10^{-3}$	26.3	45.2	39.7	38.9	-15.8	7184
$TT < -2 \times 10^{-3}$	10.9	15.3	7.6	185.6	29.5	2782

absolute EB deficit is smaller than $20 W m^{-2}$. In Section 3.10 it will be shown that absolute EB deficits smaller than $20 W m^{-2}$ can be explained by neglecting storage terms.

3.5. Multi-site analysis of EB closure as a function of the time of the day

Fig. 3 shows the relative EB deficit as a function of the time of the day, including data from all 26 sites. This pattern holds for all considered subsets of climate conditions (not shown). It is evident that the relative EB closure is improving over the course of the day during daytime, and at the end of the afternoon the relative EB deficit is clearly lower than around noon. The figure also shows that the relative EB deficit is largest during nighttime, with maxima at the transition periods at sunrise and sunset. For the different sites and different periods of the year the timing of this transition period obviously varies, but the two peaks in Fig. 3 coincide with the average transition period.

3.6. Multi-site analysis of EB closure as a function of ξ and u_*

Table 5 displays the relative EB deficit for 20 classes with different combinations of u_* and ξ . For five classes not enough data were

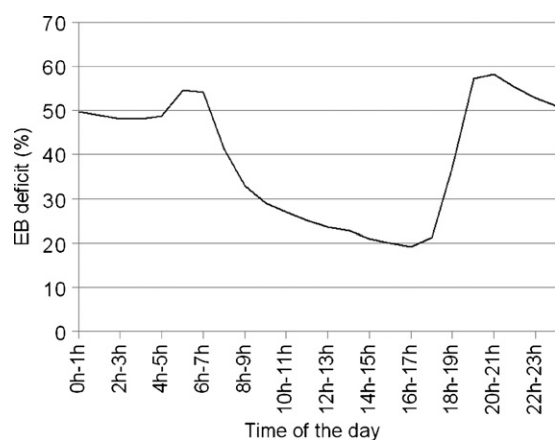


Fig. 3. The average diurnal cycle of the EB deficit (%), on the basis of 511,784 data points from 26 FLUXNET sites. The data are (almost) equally distributed over the different time periods. The uncertainty of the estimate is very small and not shown.

available. Our analysis focuses first on the results for $\xi < -0.02$. For all u_* classes, the relative EB deficit is smaller for $\xi < -1.0$ than for $-1.0 \leq \xi < -0.02$, but for two out of five u_* classes too little data are available to make a reliable estimate. The difference is only small for u_* between $0.15 m s^{-1}$ and $0.30 m s^{-1}$ (33.0% vs. 32.1%). These results suggest that the poorer relative EB closure found for very unstable atmospheric conditions (Sections 3.1 and 3.2, Table 2) is due to reduced mechanically-induced turbulence (lower u_*), because the relative EB closure is better for very unstable conditions than less unstable conditions within u_* classes. These results support the findings presented in Section 3.4. The analysis shows further that the smallest relative EB deficits are obtained for elevated u_* in combination with unstable atmospheric conditions. The largest relative EB deficits occur for stable conditions at low u_* . This analysis, on the basis of regression without offset, shows that the relative EB deficit for stable conditions, but elevated u_* , tends to be lower than for similar u_* , but at neutral atmospheric stratification. Very different results are obtained if the average EB deficit is calculated in terms of absolute values ($W m^{-2}$). In this case, the absolute EB deficit is largest for very unstable conditions and u_* ranging between $0.15 m s^{-1}$ and $0.45 m s^{-1}$ (above $75 W m^{-2}$). These conditions are associated with the highest average net radiation. Once more this shows that the conditions with the lowest relative EB deficit are often associated with the largest absolute EB deficits. The conditions with the largest relative EB deficits are in most cases associated with an absolute EB deficit smaller than $20 W m^{-2}$, which is probably not significant given the fact that the neglecting of storage can explain such a deficit (see also Section 3.10). We also derived regression equations allowing for an offset. For stable atmospheric conditions the offset is positive (as expected), and the regression slope is steeper compared to that for an analysis without offset. This can be attributed to the fact that average net radiation for stable conditions is negative for all u_* classes. Therefore the results presented in Table 5 have to be interpreted with care.

3.7. Multi-site analysis of EB closure as a function of u_* and TT

Results of this analysis are presented in Table 6. It largely confirms the results of the previous sections: the lowest relative EB deficits are found for elevated u_* and elevated positive TT values. Low u_* combined with weakly negative TT conditions present the highest relative EB deficits. Surprisingly, more strongly neg-

Table 5
Average EB deficits (in $W m^{-2}$ and in brackets in %) for 24 European FLUXNET sites and 20 classes with different combinations of u^* and ξ . The average EB deficit is estimated with help of a regression without offset. The grey shading indicates whether the relative EB deficit for a certain class (in terms of %) is large (dark grey) or low (light grey).

	$\xi < -1.0$	$-0.02 > \xi \geq -1.0$	$0.02 > \xi \geq -0.02$	$1.0 > \xi \geq 0.02$	$\xi \geq 1.0$
$u^* < 0.15 m s^{-1}$	17.5 (37.2%)	7.1 (47.3%)	-17.3 (67.0%)	-13.1 (75.1%)	-21.7 (69.7%)
$0.15 m s^{-1} \leq u^* < 0.30 m s^{-1}$	75.3 (32.1%)	46.3 (33.0%)	6.0 (39.9%)	-9.2 (54.0%)	-9.0 (33.2%)
$0.30 m s^{-1} \leq u^* < 0.45 m s^{-1}$	83.2 (22.9%)	65.2 (29.8%)	16.6 (41.3%)	5.1 (40.1%)	Few data
$0.45 m s^{-1} \leq u^* < 0.60 m s^{-1}$	Few data	67.0 (22.3%)	19.0 (40.5%)	18.0 (29.0%)	Few data
$u^* \geq 0.60 m s^{-1}$	Few data	39.3 (13.8%)	21.3 (31.1%)	29.5 (17.4%)	Few data

ative TT values (i.e., a strong inversion) result in a much better relative EB closure than neutral conditions. However, also in this case the conclusion might be affected by the regression without offset. A regression with offset shows large offset values for non-neutral conditions and especially for the largest TT values (up to $101.7 W m^{-2}$). As seen before, the largest absolute EB deficits (above $80 W m^{-2}$ on average) are expected for those conditions with the smallest relative EB deficits: elevated TT and moderate u^* ($0.30-0.60 m s^{-1}$). The absolute EB deficits are relatively small for negative TT values and TT values close to zero. In most cases the absolute EB deficit is rather insignificant under those conditions (smaller than $20 W m^{-2}$).

For positive TT (with only a limited number of cases with negative net radiation) the relative EB deficit was also calculated with the bulk method. This method gave again only meaningful results for positive TT values. The resulting EB deficits are (again) lower than those derived from the regression without offset, and drop to 14% for the class with the highest u^* and the most elevated TT.

3.8. Multi-site analysis of EB closure as function of the time of the day

The EB closure is analyzed here as a joint function of u^* , ξ (or TT) and time of the day. The disadvantage of such a trivariate analysis is that less data points are available for each of the different classes. Therefore, the uncertainty of the estimates for this analysis is larger than for those of the other subsections.

Fig. 4 shows the relative EB deficit as a function of u^* and time of the day, still irrespectively of ξ . The graph illustrates that when u^* is larger than $0.45 m s^{-1}$, the relative EB closure does not depend on the time of the day. On the other hand, for u^* below $0.30 m s^{-1}$, the relative closure is clearly poorer during nighttime.

Fig. 5 displays the relative EB deficit as a function of ξ and time of the day, irrespectively of u^* . As mentioned before, the relative EB deficit is in general larger for very unstable conditions than for (medium) unstable conditions. During daytime, the relative EB deficit is very low for very stable conditions. But these conditions occur rarely, and data from Collelongo and Renon build a large number of those cases. These two sites have in general a small EB

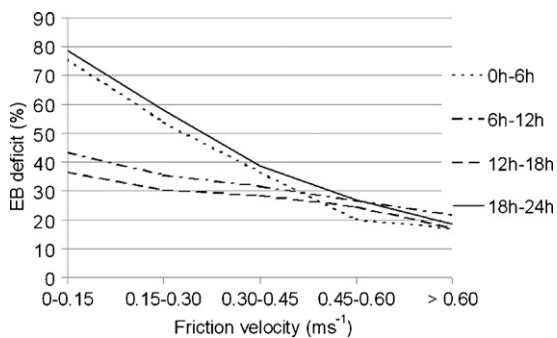


Fig. 4. EB deficit as a function of u^* , stratified for different time periods for 24 European FLUXNET stations. For all classes at least 10,000 data points were available (in half of the cases more than 20,000 data points).

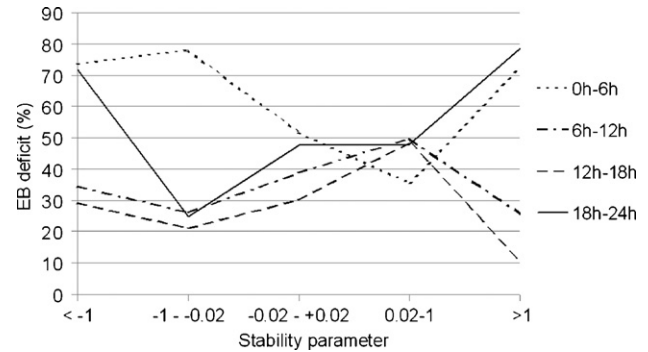


Fig. 5. EB deficit as a function of ξ , stratified for different time periods for 25 European FLUXNET stations. For all except the following classes at least 18,000 data points were available: $\xi \leq -1$ between 0 h and 6 h (5148 data points), $\xi \leq -1$ between 6 h and 12 h (9312 data points), $\xi \leq -1$ between 12 h and 18 h (5300 data points), $\xi \leq -1$ between 18 h and 24 h (4551 data points), $-0.02 \geq \xi > -1$ between 0 h and 6 h (6,089 data points), $-0.02 \geq \xi > -1$ between 18 h and 24 h (8331 data points), $\xi \geq 1$ between 6 h and 12 h (4284 data points) and $\xi \geq 1$ between 12 h and 18 h (3085 data points).

deficit for stable conditions. Both sites are located in mountainous regions at an altitude of more than 1500 m a.s.l., and maybe the improved closure is related to the fact that the sites are characterized by elevated wind velocities, also under stable conditions. The large relative EB deficit during nighttime and its relation with ξ will not be analyzed further as the large relative EB deficits are associated with small absolute EB deficits. These nocturnal EB deficits can partly be explained by storage effects (see Section 3.10).

Fig. 6 shows the relative EB deficit as a function of TT. Again we find for all time periods a smaller relative EB deficit for strongly positive TT. This confirms that the poorer closure in the univariate analysis for very unstable atmospheric conditions compared with less unstable conditions is caused by the reduced mechanically-

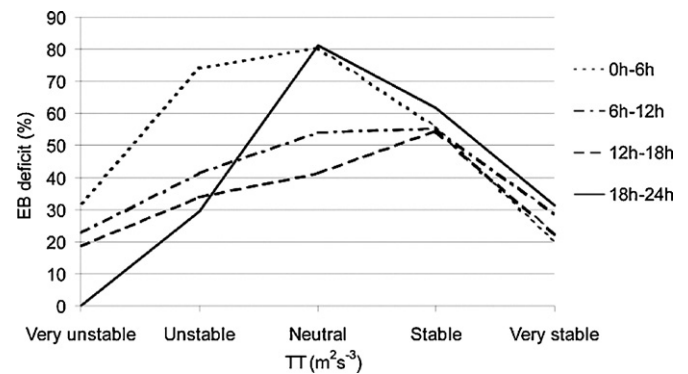


Fig. 6. EB deficit as a function of TT, stratified for different time periods and for 24 European FLUXNET stations. The classes on the horizontal axis stand for: $TT \geq 1 \times 10^{-3} m^2 s^{-3}$ (very unstable), $1 \times 10^{-4} m^2 s^{-3} \leq TT < 1 \times 10^{-3} m^2 s^{-3}$ (unstable), $-1 \times 10^{-4} m^2 s^{-3} \leq TT < 1 \times 10^{-4} m^2 s^{-3}$ (neutral), $-3 \times 10^{-4} m^2 s^{-3} \leq TT < -1 \times 10^{-4} m^2 s^{-3}$ (stable) and $TT < 3 \times 10^{-4} m^2 s^{-3}$ (very stable). For all classes at least 10,000 data points were available, except for the two classes with positive TT (i.e., the largest TT) between 0–6 h and 18–24 h.

Table 6
 Analysis on the basis of 24 European FLUXNET sites for 25 different classes of u_* and TT (a) average EB deficit on the basis of a regression without offset (%), (b) the magnitude of the offset, if a regression with offset is performed ($W m^{-2}$), (c) average net radiation ($W m^{-2}$), (d) average EB deficit ($W m^{-2}$). The grey shading indicates whether the EB deficit for a certain class (in terms of %) is large (dark grey) or low (light grey).

(a)	$TT > 10^{-3} m^2 s^{-3}$	$10^{-3} m^2 s^{-3} > TT \geq 10^{-4} m^2 s^{-3}$	$10^{-4} m^2 s^{-3} > TT \geq -10^{-4} m^2 s^{-3}$	$-10^{-4} m^2 s^{-3} > TT \geq -3 \times 10^{-4} m^2 s^{-3}$	$TT < -3 \times 10^{-4} m^2 s^{-3}$
$u_* < 0.15 m s^{-1}$	23.2	47.3	57.9	80.9	43.4
$0.15 m s^{-1} \leq u_* < 0.30 m s^{-1}$	24.7	42.0	50.9	74.3	37.4
$0.30 m s^{-1} \leq u_* < 0.45 m s^{-1}$	26.1	38.7	40.6	58.1	26.7
$0.45 m s^{-1} \leq u_* < 0.60 m s^{-1}$	23.5	34.6	34.9	42.0	17.3
$u_* \geq 0.60 m s^{-1}$	16.4	32.6	41.5	45.8	28.1
(b)	$TT > 10^{-3} m^2 s^{-3}$	$10^{-3} m^2 s^{-3} > TT \geq 10^{-4} m^2 s^{-3}$	$10^{-4} m^2 s^{-3} > TT \geq -10^{-4} m^2 s^{-3}$	$-10^{-4} m^2 s^{-3} > TT \geq -3 \times 10^{-4} m^2 s^{-3}$	$TT < -3 \times 10^{-4} m^2 s^{-3}$
$u_* < 0.15 m s^{-1}$	-35.1	-9.2	-2.5	10.2	6.2
$0.15 m s^{-1} \leq u_* < 0.30 m s^{-1}$	-62.8	-20.1	-0.6	10.7	8.6
$0.30 m s^{-1} \leq u_* < 0.45 m s^{-1}$	-87.6	-26.1	1.4	11.5	13.0
$0.45 m s^{-1} \leq u_* < 0.60 m s^{-1}$	-86.8	-29.3	1.5	12.8	18.1
$u_* \geq 0.60 m s^{-1}$	-101.7	-41.5	-3.2	16.8	31.7
(c)	$TT > 10^{-3} m^2 s^{-3}$	$10^{-3} m^2 s^{-3} > TT \geq 10^{-4} m^2 s^{-3}$	$10^{-4} m^2 s^{-3} > TT \geq -10^{-4} m^2 s^{-3}$	$-10^{-4} m^2 s^{-3} > TT \geq -3 \times 10^{-4} m^2 s^{-3}$	$TT < -3 \times 10^{-4} m^2 s^{-3}$
$u_* < 0.15 m s^{-1}$	273.2	92.9	-18.3	-33.7	-24.2
$0.15 m s^{-1} \leq u_* < 0.30 m s^{-1}$	315.9	160.9	12.1	-29.4	-30.6
$0.30 m s^{-1} \leq u_* < 0.45 m s^{-1}$	378.1	171.1	31.0	-11.4	-27.4
$0.45 m s^{-1} \leq u_* < 0.60 m s^{-1}$	420.1	163.3	33.9	0.4	-19.9
$u_* \geq 0.60 m s^{-1}$	426.5	146.2	35.8	6.7	-11.5
(d)	$TT > 10^{-3} m^2 s^{-3}$	$10^{-3} m^2 s^{-3} > TT \geq 10^{-4} m^2 s^{-3}$	$10^{-4} m^2 s^{-3} > TT \geq -10^{-4} m^2 s^{-3}$	$-10^{-4} m^2 s^{-3} > TT \geq -3 \times 10^{-4} m^2 s^{-3}$	$TT < -3 \times 10^{-4} m^2 s^{-3}$
$u_* < 0.15 m s^{-1}$	52.1	38.3	-14.7	-17.0	-4.5
$0.15 m s^{-1} \leq u_* < 0.30 m s^{-1}$	61.5	58.7	6.0	-11.4	-4.3
$0.30 m s^{-1} \leq u_* < 0.45 m s^{-1}$	83.5	56.2	14.5	4.8	4.2
$0.45 m s^{-1} \leq u_* < 0.60 m s^{-1}$	86.0	44.7	14.0	13.0	13.6
$u_* \geq 0.60 m s^{-1}$	54.5	30.2	13.0	19.8	28.3

Table 7
Average EB deficits (in $W m^{-2}$ and in brackets in %) for 24 European FLUXNET sites for four different time periods and 25 classes with different combinations of u_* and ξ . If the number of measurement data was smaller than 1000, no value is given because the uncertainty of the estimate is considerable. The grey shading indicates whether the EB deficit for a certain class (in terms of %) is large (dark grey) or low (light grey). (a) EB deficits for 0–6 h, (b) for 6–12 h, (c) 12–18 h, and (d) 18–24 h.

(a) 0–6 h	$\xi < -1.0$	$-0.02 > \xi \geq -1.0$	$0.02 > \xi \geq -0.02$	$1.0 > \xi \geq 0.02$	$\xi \geq 1.0$
$u_* < 0.15 m s^{-1}$	-20.3 (85.4%)	-13.1 (84.7%)	-20.8 (77.9%)	-14.5 (72.8%)	-21.3 (74.8%)
$0.15 m s^{-1} \leq u_* < 0.30 m s^{-1}$	Few data	-6.8 (75.5%)	-5.4 (80.3%)	10.3 (51.8%)	-13.6 (48.2%)
$0.30 m s^{-1} \leq u_* < 0.45 m s^{-1}$	Few data	-16.1 (64.7%)	0.2 (80.0%)	-0.1 (30.0%)	Few data
$0.45 m s^{-1} \leq u_* < 0.60 m s^{-1}$	Few data	Few data	1.6 (49.3%)	8.5 (15.3%)	Few data
$u_* \geq 0.60 m s^{-1}$	Few data	Few data	21.0 (33.5%)	18.5 (0.9%)	Few data
(b) 6–12 h	$\xi < -1.0$	$-0.02 > \xi \geq -1.0$	$0.02 > \xi \geq -0.02$	$1.0 > \xi \geq 0.02$	$\xi \geq 1.0$
$u_* < 0.15 m s^{-1}$	66.5 (39.0%)	45.4 (51.0%)	Few data	18.6 (77.2%)	20.1 (53.1%)
$0.15 m s^{-1} \leq u_* < 0.30 m s^{-1}$	95.3 (33.0%)	67.5 (35.9%)	30.3 (44.3%)	22.6 (72.0%)	58.8 (30.3%)
$0.30 m s^{-1} \leq u_* < 0.45 m s^{-1}$	100.3 (24.4%)	81.1 (31.6%)	37.5 (46.0%)	30.5 (42.6%)	Few data
$0.45 m s^{-1} \leq u_* < 0.60 m s^{-1}$	Few data	83.3 (38.7%)	37.1 (38.7%)	38.1 (41.4%)	Few data
$u_* \geq 0.60 m s^{-1}$	Few data	70.4 (20.1%)	36.5 (37.4%)	43.9 (31.5%)	Few data
(c) 12–18 h	$\xi < -1.0$	$-0.02 > \xi \geq -1.0$	$0.02 > \xi \geq -0.02$	$1.0 > \xi \geq 0.02$	$\xi \geq 1.0$
$u_* < 0.15 m s^{-1}$	49.7 (29.7%)	28.6 (35.4%)	Few data	1.6 (75.5%)	-1.7 (58.6%)
$0.15 m s^{-1} \leq u_* < 0.30 m s^{-1}$	79.1 (30.6%)	40.4 (27.8%)	10.7 (27.0%)	12.2 (61.3%)	Few data
$0.30 m s^{-1} \leq u_* < 0.45 m s^{-1}$	91.8 (23.1%)	58.6 (29.0%)	22.4 (33.4%)	21.5 (51.5%)	Few data
$0.45 m s^{-1} \leq u_* < 0.60 m s^{-1}$	Few data	65.6 (24.8%)	26.3 (33.5%)	26.6 (42.1%)	Few data
$u_* \geq 0.60 m s^{-1}$	Few data	49.7 (16.3%)	30.1 (31.3%)	39.8 (29.0%)	Few data
(d) 18–24 h	$\xi < -1.0$	$-0.02 > \xi \geq -1.0$	$0.02 > \xi \geq -0.02$	$1.0 > \xi \geq 0.02$	$\xi \geq 1.0$
$u_* < 0.15 m s^{-1}$	-33.6 (84.9%)	-26.5 (71.0%)	-30.9 (81.3%)	-22.0 (75.9%)	-31.2 (80.4%)
$0.15 m s^{-1} \leq u_* < 0.30 m s^{-1}$	Few data	-28.1 (46.1%)	-15.4 (69.1%)	-13.5 (59.2%)	-17.2 (59.3%)
$0.30 m s^{-1} \leq u_* < 0.45 m s^{-1}$	Few data	-17.7 (22.7%)	-5.4 (57.4%)	-7.4 (40.6%)	Few data
$0.45 m s^{-1} \leq u_* < 0.60 m s^{-1}$	Few data	-26.2 (12.4%)	-5.0 (48.2%)	2.1 (29.7%)	Few data
$u_* \geq 0.60 m s^{-1}$	Few data	-71.2 (0.0%)	1.9 (32.4%)	14.7 (12.7%)	Few data

induced turbulence (lower u_*). Surprisingly, the relative closure is poorest for TT values close to zero, whereas negative TT values (i.e., inversion conditions) are associated with an improved closure. The analysis shows that the relative EB closure is smallest for strongly positive or strongly negative TT. The fact that this result is more pronounced for the analysis in terms of TT than in terms of ξ , might be again related to the fact that ξ is both impacted by u_* as well as TT. Very stable conditions are a combination of low mechanically-induced turbulence and strongly negative TT. The low mechanically-induced turbulence is associated with large EB deficits, but the sole impact of TT seems to yield larger relative EB deficits for values close to zero, and smaller relative deficits for large absolute TT values. Moreover, it is important to notice that for the cases with a negative TT the differences in relative EB closure between nighttime and daytime are very small. In general, the differences in EB closure between daytime and nighttime are smaller if the analysis is made with relative EB deficit as a function of TT compared to an analysis as a function of ξ .

Table 7 shows for four different time periods (0–6 h, 6–12 h, 12–18 h, 18–24 h) the relative and absolute EB deficit as a function of u_* and ξ . The number of data points did not allow a very detailed analysis for many classes. We focus on the results for the periods that mostly coincide with daytime (the time blocks of 6–12 h and 12–18 h). For 15 out of the 18 u_* - ξ classes that could be analyzed, the relative EB deficit is larger during the morning than during the afternoon. Irrespectively of u_* and ξ , the relative EB deficit is around 6 percentage points larger for the 6–12 h time period than for the 12–18 h time period. We will see later in Section 3.10 that this difference is partly related to the energy storage between the EC sensors and the soil heat flux plate; it is also partly related to increased turbulent mixing in the afternoon. The relative EB deficit is smaller for very unstable conditions than for less unstable conditions, once more confirming that the poorer relative EB deficit for very unstable conditions in the univariate analysis is related with the reduced mechanically-induced turbulence under those conditions. For relatively low u_* , the relative EB deficit is larger for neutral

and stable compared to unstable conditions. For elevated u_* , differences in relative EB closure between unstable, neutral and stable conditions are smaller. These results have to be considered with some caution as for non-neutral conditions the relative EB deficit does not correspond exactly to the slope of the regression equation (Section 2.2). Our regressions with offsets revealed intercepts of up to $40 W m^{-2}$ for stable conditions (the intercept is a function of the u_* , with larger intercepts for elevated u_*) and below $-100 W m^{-2}$ in extreme cases under unstable conditions (again for conditions with elevated u_*). Estimates of the relative EB deficit derived using the bulk method indicated once more that regression without offset overestimates the relative EB deficit for unstable conditions.

It is also important to investigate the absolute EB deficits as a function of the three variables. During nighttime, absolute EB deficits are in most cases small (below $20 W m^{-2}$). During daytime the largest absolute EB deficits nearly coincide with the conditions with the smallest relative EB deficits: (very) unstable conditions and moderately high u_* (0.30 – $0.45 m s^{-1}$). However, compared to the conditions with the smallest relative EB deficit there is a small shift: the absolute EB deficits are slightly larger in the morning than in the afternoon and larger for moderate u_* (around $0.45 m s^{-1}$) than for higher u_* ($>0.60 m s^{-1}$). For very unstable conditions during the period 6–12 h and u_* between $0.30 m s^{-1}$ and $0.45 m s^{-1}$, the average EB deficit is $100.3 W m^{-2}$. For neutral and stable conditions during daytime the absolute EB deficit is in all cases, except two, smaller than $40 W m^{-2}$, and in some cases (small u_*) even smaller than $20 W m^{-2}$. Also here we find a fundamental difference between relative and absolute EB deficits: during daytime the conditions with the largest relative EB deficits are associated with absolute EB deficits that are on the borderline of being insignificant.

Table 8 presents an analysis of the EB deficit as a function of u_* and TT. Again relative EB closure improves for increased u_* and increased TT values. The poorest relative EB closure is found for conditions with TT values close to zero or slightly negative. Conditions with an elevated negative TT (i.e., very stable atmospheric conditions) are associated with a limited relative EB deficit. The largest

Table 8
Average EB deficits (%) for 24 European FLUXNET sites for four different time periods and 25 classes with different combinations of u_* and TT (denominator of Eq. (5)). If the number of measurement data was smaller than 1000, no value is given because the uncertainty of the estimate is considerable. The grey shading indicates whether the EB deficit for a certain class (in terms of %) is large (dark grey) or low (light grey). (a) EB deficits for 0–6 h, (b) for 6–12 h, (c) 12–18 h, and (d) 18–24 h.

(a) 0–6 h	$TT > 10^{-3} \text{ m}^2 \text{ s}^{-3}$	$10^{-3} \text{ m}^2 \text{ s}^{-3} > TT \geq 10^{-4} \text{ m}^2 \text{ s}^{-3}$	$10^{-4} \text{ m}^2 \text{ s}^{-3} > TT \geq -10^{-4} \text{ m}^2 \text{ s}^{-3}$	$-10^{-4} \text{ m}^2 \text{ s}^{-3} > TT \geq -3 \times 10^{-4} \text{ m}^2 \text{ s}^{-3}$	$TT < -3 \times 10^{-4} \text{ m}^2 \text{ s}^{-3}$
$u_* < 0.15 \text{ m s}^{-1}$	Few data	12.0 (76.8%)	-19.0 (80.9%)	-17.0 (66.2%)	-6.1 (45.0%)
$0.15 \text{ m s}^{-1} \leq u_* < 0.30 \text{ m s}^{-1}$	Few data	-9.5 (70.3%)	-7.1 (78.5%)	-14.4 (56.5%)	-6.4 (36.0%)
$0.30 \text{ m s}^{-1} \leq u_* < 0.45 \text{ m s}^{-1}$	Few data	-16.3 (63.5%)	-2.2 (76.0%)	-0.7 (40.6%)	0.9 (22.7%)
$0.45 \text{ m s}^{-1} \leq u_* < 0.60 \text{ m s}^{-1}$	Few data	-24.0 (62.4%)	-3.2 (78.1%)	7.1 (34.9%)	10.1 (11.8%)
$u_* \geq 0.60 \text{ m s}^{-1}$	Few data	-42.1 (92.1%)	-10.2 (82.9%)	9.2 (37.5%)	21.5 (0.7%)
(b) 6–12 h	$TT > 10^{-3} \text{ m}^2 \text{ s}^{-3}$	$10^{-3} \text{ m}^2 \text{ s}^{-3} > TT \geq 10^{-4} \text{ m}^2 \text{ s}^{-3}$	$10^{-4} \text{ m}^2 \text{ s}^{-3} > TT \geq -10^{-4} \text{ m}^2 \text{ s}^{-3}$	$-10^{-4} \text{ m}^2 \text{ s}^{-3} > TT \geq -3 \times 10^{-4} \text{ m}^2 \text{ s}^{-3}$	$TT < -3 \times 10^{-4} \text{ m}^2 \text{ s}^{-3}$
$u_* < 0.15 \text{ m s}^{-1}$	66.0 (26.1%)	65.4 (51.9%)	31.0 (59.1%)	12.4 (72.9%)	Few data
$0.15 \text{ m s}^{-1} \leq u_* < 0.30 \text{ m s}^{-1}$	79.1 (26.5%)	78.8 (44.6%)	35.4 (60.7%)	18.1 (75.3%)	33.8 (33.1%)
$0.30 \text{ m s}^{-1} \leq u_* < 0.45 \text{ m s}^{-1}$	95.0 (27.2%)	74.7 (40.9%)	36.6 (47.1%)	27.9 (48.5%)	37.4 (24.6%)
$0.45 \text{ m s}^{-1} \leq u_* < 0.60 \text{ m s}^{-1}$	97.1 (24.1%)	62.6 (37.4%)	35.0 (39.8%)	34.1 (44.0%)	42.3 (23.3%)
$u_* \geq 0.60 \text{ m s}^{-1}$	71.1 (18.6%)	48.6 (36.5%)	30.4 (49.8%)	37.0 (52.8%)	46.0 (33.3%)
(c) 12–18 h	$TT > 10^{-3} \text{ m}^2 \text{ s}^{-3}$	$10^{-3} \text{ m}^2 \text{ s}^{-3} > TT \geq 10^{-4} \text{ m}^2 \text{ s}^{-3}$	$10^{-4} \text{ m}^2 \text{ s}^{-3} > TT \geq -10^{-4} \text{ m}^2 \text{ s}^{-3}$	$-10^{-4} \text{ m}^2 \text{ s}^{-3} > TT \geq -3 \times 10^{-4} \text{ m}^2 \text{ s}^{-3}$	$TT < -3 \times 10^{-4} \text{ m}^2 \text{ s}^{-3}$
$u_* < 0.15 \text{ m s}^{-1}$	48.3 (18.7%)	51.0 (40.8%)	7.9 (52.8%)	4.5 (70.8%)	Few data
$0.15 \text{ m s}^{-1} \leq u_* < 0.30 \text{ m s}^{-1}$	53.9 (22.1%)	51.0 (37.1%)	16.5 (40.6%)	9.2 (68.4%)	14.9 (34.8%)
$0.30 \text{ m s}^{-1} \leq u_* < 0.45 \text{ m s}^{-1}$	75.4 (24.7%)	51.8 (35.8%)	21.1 (36.2%)	20.7 (57.1%)	22.4 (22.3%)
$0.45 \text{ m s}^{-1} \leq u_* < 0.60 \text{ m s}^{-1}$	80.8 (23.0%)	45.0 (32.2%)	21.8 (33.2%)	24.5 (42.9%)	24.2 (12.6%)
$u_* \geq 0.60 \text{ m s}^{-1}$	50.5 (15.4%)	33.6 (30.0%)	26.4 (38.2%)	34.1 (45.1%)	41.5 (25.8%)
(d) 18–24 h	$TT > 10^{-3} \text{ m}^2 \text{ s}^{-3}$	$10^{-3} \text{ m}^2 \text{ s}^{-3} > TT \geq 10^{-4} \text{ m}^2 \text{ s}^{-3}$	$10^{-4} \text{ m}^2 \text{ s}^{-3} > TT \geq -10^{-4} \text{ m}^2 \text{ s}^{-3}$	$-10^{-4} \text{ m}^2 \text{ s}^{-3} > TT \geq -3 \times 10^{-4} \text{ m}^2 \text{ s}^{-3}$	$TT < -3 \times 10^{-4} \text{ m}^2 \text{ s}^{-3}$
$u_* < 0.15 \text{ m s}^{-1}$	Few data	-24.7 (57.8%)	-29.6 (84.2%)	-24.4 (69.9%)	-11.3 (57.6%)
$0.15 \text{ m s}^{-1} \leq u_* < 0.30 \text{ m s}^{-1}$	Few data	-19.3 (38.8%)	-14.3 (75.4%)	-21.2 (63.9%)	-13.7 (45.2%)
$0.30 \text{ m s}^{-1} \leq u_* < 0.45 \text{ m s}^{-1}$	Few data	-19.3 (24.6%)	-6.8 (66.9%)	-7.4 (51.0%)	-6.8 (36.0%)
$0.45 \text{ m s}^{-1} \leq u_* < 0.60 \text{ m s}^{-1}$	Few data	-20.4 (21.0%)	-9.0 (60.1%)	0.1 (50.3%)	3.4 (25.6%)
$u_* \geq 0.60 \text{ m s}^{-1}$	Few data	-40.7 (24.6%)	-13.6 (65.7%)	4.3 (48.1%)	17.3 (12.6%)

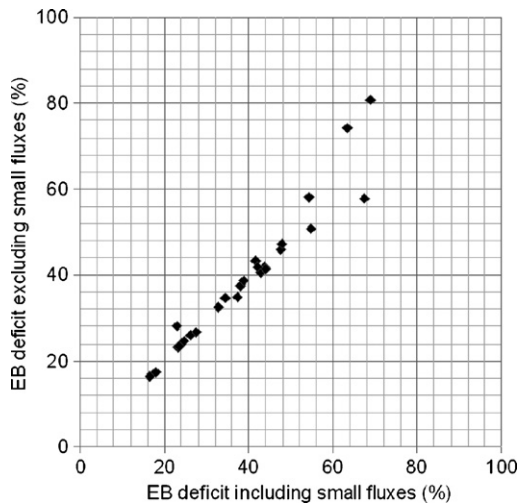


Fig. 7. Analysis on the basis of 24 European FLUXNET sites for 25 different classes of u^* and TT. Compared are EB deficits with and without excluding the cases with an absolute net radiation $< 50 \text{ W m}^{-2}$.

absolute EB deficits are found for (elevated) positive TT values, moderate u^* ($0.30\text{--}0.60 \text{ m s}^{-1}$), and during daytime (with poorer closure during the morning than in the afternoon). An analysis of relative EB deficit as a function of u^* and TT compared to an analysis in terms of u^* and ξ , shows less difference between nighttime and daytime.

3.9. The role of small turbulent fluxes for the overall relative EB closure

Although differences in relative EB closure between daytime and nighttime can be partly explained by u^* and TT (Section 3.8), part of these differences remain unexplained. The conditions for which relative EB closure is poor are in general associated with small turbulent flux densities and small negative net radiation. It is likely that small, systematic measurement errors and the neglecting of the storage term enhance the relative EB deficit. The poor relative EB closure during nighttime is associated with small errors for the absolute EB deficit. Therefore the analysis of the relative EB deficit was repeated leaving out all cases with an absolute net radiation smaller than 50 W m^{-2} in order to find out whether the relative EB closure would improve for these conditions. The relative EB deficit was determined in these cases as the slope of the regression equation, fixing the intercept of the regression equation at the origin. The results are compared with a similar regression that does not exclude the small fluxes. The results for both regressions are calculated for the 25 combinations of u^* and TT presented in Section 3.7 (Fig. 7). The neglecting of small fluxes does not reduce the relative EB deficit (39.3% vs. 39.6% with and without including the small fluxes, respectively, averaged over the 25 cases). The question was further explored by focusing on those cases of Section 3.8 which had a relative EB deficit larger than 50%. Leaving out the small fluxes for those cases does not significantly modify the relative EB deficit; actually, the relative EB deficit is often even somewhat larger when small fluxes are not considered.

3.10. The role of storage terms

In order to investigate the role of storage terms, the overall EB closure was calculated for six sites (Vielsalm, Tharandt, Brasschaat, Castel Porziano, Loobos and Collelongo) including ΔS_{LE} and ΔS_H . These results are compared with those excluding storage in Table 9. Including ΔS_{LE} and ΔS_H improves the relative EB closure only up

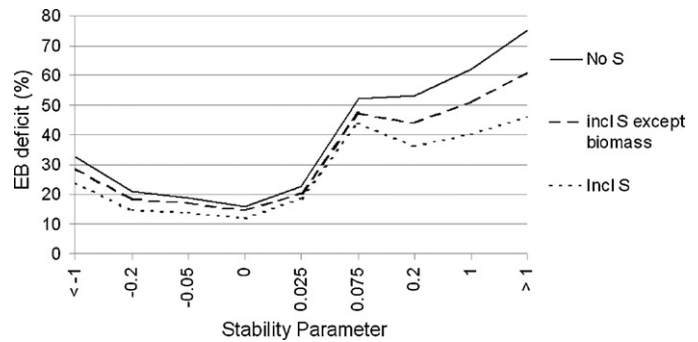


Fig. 8. EB deficit as a function of ξ , for three different analyses that exclude storage terms (No S), that include ΔS_H and ΔS_{LE} (including S except biomass) and that include also ΔS_{BIO} (including S). The analyses were made including data from the sites Vielsalm and Tharandt with at least 3721 data points per ξ class and on average around 9700 data points per class. The upper boundary of the ξ class is given, the lower boundary value is given by the preceding value (for instance: -0.2 stands for the class with stabilities between -1.0 and -0.2).

to 0.7 percentage points for four of the six sites, but for two of the sites with the tallest vegetation the reduction of the relative EB deficit is of 2.0 (Tharandt) and 3.1 (Vielsalm) percentage points when including ΔS_{LE} and ΔS_H . For Vielsalm and Tharandt including in addition ΔS_{BIO} improves the relative EB closure significantly, and its contribution is larger than for ΔS_{LE} and ΔS_H . For these two sites ΔS_{BIO} accounts for more than 60% of the relative EB deficit reduction achieved by including the three storage terms. If we assume that this relation is similar for the other sites, we would find for the six sites an average relative EB deficit including the three storage terms of 22.0%, whereas it is 25.6% without including the storage term. Note that for the sites with smaller vegetation the impact of the storage terms is smaller than for the sites with tall vegetation. For the 26 sites we estimate that the storage term accounts for a reduction of the relative EB deficit of 2.5 percentage points, taking into account that the average sensor height for the six sites was 33 m and therefore higher than the average sensor height over all 26 sites (23 m).

For the present investigation, the impact of neglecting storage for the inferred relationships between environmental conditions and EB closure is more important than its absolute mean quantitative effect on EB closure. These aspects are discussed in more detail in the following paragraphs.

The relation between EB deficit and ξ is analyzed first on the basis of a multi-site analysis using data from all six sites, and comparing the results excluding all storage terms with an analysis including ΔS_{LE} and ΔS_H . The differences between the two analyses are very small for unstable and neutral conditions, both for relative and absolute EB deficits (for all categories smaller than 2 percentage points and smaller than 6 W m^{-2}). For stable conditions the differences are larger for relative EB deficits: for very stable atmospheric conditions ($\xi > 1$) the EB deficit was 12 percentage points smaller if ΔS_{LE} and ΔS_H were included (36.5% vs. 48.6%) (not shown). A separate analysis to look at the role of ΔS_{BIO} was also made, considering only the sites Vielsalm and Tharandt. Fig. 8 shows the relation between ξ and relative EB deficit for these two sites. The figure illustrates that the relation between the relative EB deficit and ξ is not altered by the inclusion of the storage term, but for stable conditions the storage terms result in an important reduction of the relative EB deficit, whereas this reduction is much smaller for unstable and neutral conditions. The absolute EB deficits are also smaller if storage terms are considered, and only larger than 20 W m^{-2} for unstable conditions. The largest absolute EB deficits are again found for unstable conditions (37.5 W m^{-2} for moderately unstable conditions). Tharandt and Vielsalm are among the sites with highest sensor heights (42 m and 40 m, respectively)

Table 9

Average EB deficits (%) for 6 European FLUXNET sites, excluding all storage terms, including ΔS_H and ΔS_{LE} , and including ΔS_H , ΔS_{LE} and ΔS_{BIO} . In brackets the number of data points is given.

Site	EB deficit (excluding all storage terms)	EB deficit (excluding biomass storage)	EB deficit (including three storage terms)
Brasschaat	34.4 (n = 23347)	35.8 (n = 6120)	36.0 (n = 4064)
Castel-Porziano	31.1 (n = 27453)	30.4 (n = 27441)	
Collelongo	32.4 (n = 5913)	31.8 (n = 5854)	
Loobos	17.2 (n = 30535)	16.8 (n = 22437)	
Tharandt	19.4 (n = 63148)	17.4 (n = 61930)	13.9 (n = 61194)
Vielsalm	27.8 (n = 25622)	24.7 (n = 24819)	20.1 (n = 24817)

and as the average sensor height (over all 26 sites) is 23 m it is assumed that on average the storage term ($\Delta S_H + \Delta S_{LE} + \Delta S_{BIO}$) is only about half as large as found for Tharandt and Vielsalm.

The analyses of the relative and absolute EB deficit as a function of the time of the day, for scenarios that include or exclude storage terms, are in line with the results reported before. Fig. 9 shows that the differences are small. Limiting the analysis to two sites, and analyzing the role of ΔS_{BIO} , shows that relative nocturnal EB deficit can be reduced strongly including also ΔS_{BIO} . During the afternoon the differences are small. The largest absolute EB deficits are found in the morning and afternoon, also if all storage terms are included. However, for these two sites the absolute EB deficit during the mornings (8–12 h) is reduced from 52.7 W m^{-2} to 32.3 W m^{-2} .

Not enough data are available to make a detailed analysis of relative and absolute EB deficits as a function of multiple variables. However, an analysis of the relative or absolute EB deficit as function of both the time of the day and ξ also does not give qualitatively different results as compared with an analysis that excludes the storage terms (not shown). These results hence suggest that the main conclusions from the former sections would remain valid also if the storage terms were available at all sites and included in the analysis. Nonetheless, for those sites with storage terms, including storage terms reduces the relative EB deficits, only slightly during daytime, but strongly during nighttime. The absolute EB deficits are more strongly reduced in the mornings, but are still much larger during daytime (and unstable conditions) than during nighttime and stable conditions.

To conclude, neglecting storage terms did not change the relation between the relative (or absolute) EB deficit and ξ or time of the day. The main conclusions of this paper (focused on neutral and (very) unstable conditions during daytime) are thus likely not affected by the neglecting of the storage term. Further indications that the storage term does not play a major role are: (1) relative EB deficits determined for sites with tall vs. short vegetation do not significantly differ (25.9% vs. 25.6%), (2) for single sites the EB deficit determined over the complete time series by

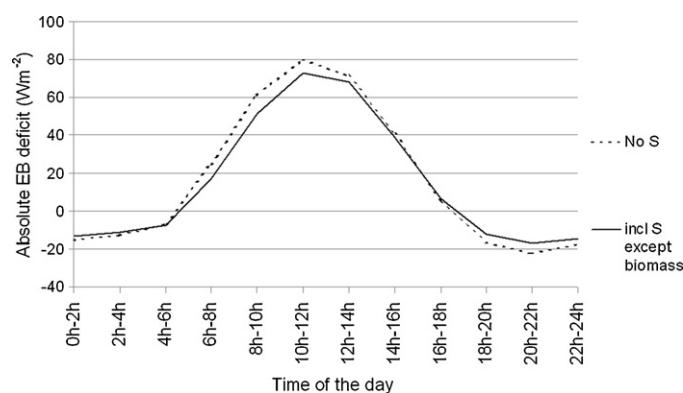


Fig. 9. Average diurnal cycle of the absolute EB deficit (W m^{-2}), excluding storage terms (No S) and including ΔS_H and ΔS_{LE} (including S except biomass) on the basis of 148,600 data points from 6 FLUXNET sites. The data are (almost) equally distributed over the different time periods.

$\sum(Q_H + Q_E) / \sum(R_n - Q_C)$ is not much smaller than the regression based EB deficits for the single measurement values (23.4% vs. 25.8%), (3) excluding cases with small net radiation from analyses does not improve the relative EB closure (39.3% for including the small fluxes and 39.6% for excluding the small fluxes), and (4) the difference between the relative EB deficit for the very early afternoon (positive storage) and the late afternoon (zero or negative storage) is only small.

3.11. Further discussion

Although this analysis does not find a higher relative EB deficit for very unstable atmospheric conditions compared with stable conditions, and after excluding the role of u_* , it is still possible that low frequency turbulence or induced meso-scale circulations would be detectable in the form of poorer relative EB closure under some conditions. It is unclear how well ξ determined at the flux towers is correlated with the regional-scale ξ . Maybe organized convection on a larger spatial scale is responsible for the poorer closure (see also Mauder et al., 2008). The correlation of EB deficits calculated at flux towers and ξ estimated from radio soundings could shed light on this question. Graf et al. (2010) recently pointed out that the non-local boundary layer profile of potential temperature affects some statistics (in particular, extremes and moments of higher than second order) more than ξ which is based on covariance values. This could also affect the energy balance closure. It would also be useful to investigate the role of ambient conditions such as ξ and wind velocity as a function of the degree of heterogeneity around a measurement site, as there are strong indications that landscape heterogeneity exercises a major control on the relative EB deficit (e.g., Mauder et al., 2007).

4. Conclusions

The main findings of this study can be summarized as follows:

- Both an analysis for 24 individual European FLUXNET sites and a multi-site analysis show that on average the relative EB deficit is larger for very unstable conditions ($\xi < -1.0$) compared with less unstable conditions ($-1.0 \leq \xi \leq -0.2$). These results are consistent with those obtained by Barr et al. (2006) for three boreal forest sites.
- A multi-site analysis of relative EB deficit as function of (1) ξ and u_* or (2) TT and u_* indicates that the larger relative EB deficit for very unstable conditions is due to the reduced mechanically-induced turbulence (low u_*) under those conditions, and not with the increased thermally-induced turbulence (TT).
- An analysis of the relative EB deficit as a function of TT, u_* and time of the day shows that the largest relative EB deficits are found for TT close to zero, and smaller deficits for $TT \gg 0$ or $TT \ll 0$. This indicates that the poor closure for very stable conditions ($\xi > 1.0$) is mainly due to low mechanically-induced turbulence (low u_*).
- It is a common procedure to estimate the relative EB deficit as the slope of the regression line of the absolute EB deficit as a function of net radiation using no offsets. However, the regression

offset is not equal to zero for non-neutral atmospheric conditions, and the slope does not correspond to the relative EB deficit for these conditions. Estimating the relative EB deficit with the bulk method is not a good alternative under many conditions.

- The average *absolute* EB deficits are largest during daytime and unstable atmospheric conditions with a moderate u_* , corresponding with the conditions with the smallest *relative* EB deficits. The conditions with the largest relative EB deficits (nighttime, low u_* , stable conditions) are associated with relatively small absolute EB deficits that could be explained by storage effects.
- Only part of the sites also recorded the storage terms for this analysis period. An analysis for this subset of sites indicates that storage terms do not play a major role for the overall closure of the energy balance, and the closure during daytime and neutral or unstable conditions. However, the EB closure during nighttime and stable conditions is significantly improved when considering storage.
- A common procedure to reduce problems with the relative EB closure consists of eliminating observations with a (very) low u_* (so-called “ u_* filtering”, e.g., Aubinet et al., 2000). While our results confirm the importance of u_* for identifying cases of poor EB closure, our analysis reveals complex relationships of EB closure with several other environmental factors, in particular the overall stability ξ , the thermally-induced turbulence TT , and the time of the day.

Acknowledgements

We would like to acknowledge the coordinating efforts by the CarboEurope IP and thank especially the PIs and their collaborators from the 26 FLUXNET sites considered in this study for access to the analyzed data. Without their continued efforts this study would not have been possible. We are also thankful to the reviewers and editor (Timothy Griffis), who helped to improve this manuscript considerably. In addition, we thank especially Alexander Graf, and also Dennis Baldocchi, Thomas Foken, Markus Reichstein, Anders Lindroth and Dario Papale for useful comments. Partial financial support was received from the EU 7th Framework Programme GENESIS Project No. 226536 and the CCES project MAIOLICA.

References

- Aubinet, M., Grelle, A., Ibrom, A., Rannik, Ü., Moncrieff, J.B., Foken, T., Kowalski, A.S., Martin, P.H., Berbigier, P., Bernhofer, C., Clement, R., Elbers, J.A., Granier, A., Grünwald, T., Morgenstern, K., Pilegaard, K., Rebmann, C., Snijders, W., Valentini, R., Vesala, T., 2000. Estimates of the annual net carbon and water exchange of European forests: the EUROFLUX methodology. *Adv. Ecol. Res.* 30, 113–175.
- Aubinet, M., Chermanne, B., Vandenhaute, M., Longdoz, B., Yernaux, M., Laitat, E., 2001. Long term carbon dioxide exchange above a mixed forest in the Belgian Ardennes. *Agr. Forest Meteorol.* 108, 293–315.
- Baldocchi, D.D., Falge, E., Gu, L., Olson, R., Hollinger, D., Running, S., Anthoni, P., Bernhofer, Ch., Davis, K., Fuentes, J., Goldstein, A., Katul, G., Law, B., Lee, X., Malhi, Y., Meyers, T., Munger, J.W., Oechel, W., Pilegaard, K., Schmid, H.P., Valentini, R., Verma, S., Vesala, T., Wilson, R., Wofsy, S., 2001. FLUXNET: a new tool to study the temporal and spatial variability of ecosystem-scale carbon dioxide, water vapor and energy flux densities. *Bull. Am. Meteorol. Soc.* 82, 2415–2435.
- Baldocchi, D.D., Wilson, K.B., 2001. Modeling CO₂ and water vapor exchange of a temperate broadleaved forest across hourly to decadal time scales. *Ecol. Model.* 142 (1–2), 155–184. doi:10.1016/S0304-3800(01)00287-3.
- Barr, A.G., Morgenstern, K., Black, T.A., McCaughey, J.H., Nesic, Z., 2006. Surface energy balance closure by the eddy-covariance method above three boreal forest stands and implications for the measurement of the CO₂ flux. *Agric. Forest Meteorol.* 140 (1–4), 322–337.
- Dolman, A.J., Moors, E.J., Elbers, J.A., 2002. The carbon uptake of a mid latitude pine forest growing on sandy soil. *Agric. Forest Meteorol.* 111, 157–170.
- Don, A., Rebmann, C., Kolle, O., Scherer-Lorenzen, M., Schulze, E.-D., 2009. Impact of afforestation-associated management changes on the carbon balance of grassland. *Glob. Change Biol.* 15, 1990–2002.
- Falge, E., Baldocchi, D., Olson, R., Anthoni, P., Aubinet, M., Bernhofer, C., Burba, G., Ceulemans, R., Clement, R., Dolman, H., Granier, A., Gross, P., Grünwald, T., Hollinger, D., Jensen, N.-O., Katul, G., Keronen, P., Kowalski, A., Lai, C.-T., Law, B.E., Meyers, T., Moncrieff, J., Moors, E., Munger, J.W., Pilegaard, K., Rannik, U., Rebmann, C., Suyker, A., Tenhunen, J., Tu, K., Verma, S., Vesala, T., Wilson, K., Wofsy, S., 2001. Gap filling strategies for long term energy flux data sets. *Agricultural and Forest Meteorology* 107 (1), 71–77.
- Finnigan, J.J., Clement, R., Malhi, Y., Leuning, R., Cleugh, H.A., 2003. A re-evaluation of long-term flux measurement techniques. Part 1: Averaging and coordinate rotation. *Bound.-Layer Meteorol.* 107, 1–48.
- Foken, T., Wimmer, F., Mauder, M., Thomas, C., Liebethal, C., 2006. Some aspects of the energy balance closure problem. *Atmos. Chem. Phys.* 6, 4395–4402.
- Foken, T., 2008. The energy balance closure problem—an overview. *Ecol. Appl.* 18 (6), 1351–1367.
- Friedlingstein, P., Cox, P., Betts, R., Bopp, L., Von Bloh, W., Brovkin, V., Cadule, P., Doney, S., Eby, M., Fung, I., Bala, G., John, J., Jones, C., Joos, F., Kato, T., Kawamiya, M., Knorr, W., Lindsay, K., Matthews, H.D., Raddatz, T., Rayner, P., Reick, C., Roeckner, E., Schnitzler, K.G., Schnur, R., Strassmann, K., Weaver, A.J., Yoshikawa, C., Zeng, N., 2006. Climate-carbon cycle feedback analysis: results from the C⁴MIP model intercomparison. *J. Climate* 19, 3337–3353.
- Gielen, B., Verbeeck, H., Neiryck, J., Sampson, D.A., Vermeiren, F., Janssens, I.A., 2010. Decadal water balance of a temperate Scots pine forest (*Pinus sylvestris* L.) based on measurements and modeling. *Biogeosciences* 7, 1247–1261.
- Gilmanov, T.G., Soussana, J.F., Aires, L., Allard, V., Ammann, C., Balzarolo, M., Barcza, Z., Bernhofer, C., Campbell, C.L., Cernusca, A., Cescatti, A., Clifton-Brown, J., Dirks, B.O.M., Dore, S., Eugste, W., Fuhrer, S.J., Gimeno, C., Gruenwald, T., Haszpra, L., Hensen, A., Ibrom, A., Jacobs, A.F.G., Jones, M.B., Lanigan, G., Laurila, T., Lohila, A., Manca, G., Marcolla, B., Nagy, Z., Pilegaard, K., Pinter, K., Pio, C., Raschi, A., Rogiers, N., Sanz, M.J., Stefan, M., Sutton, M., Tubo, Z., Valentini, R., Williams, M.L., Wohlfahrt, G., 2007. Partitioning European grassland net ecosystem CO₂ exchange into gross primary productivity and ecosystem respiration using light response function analysis. *Agric. Ecosyst. Environ.* 121 (1–2), 93–120.
- Göckede, M., Foken, T., Aubinet, M., Aurela, M., Banja, J., Bernhofer, C., Bonnefond, J.M., Brunet, Y., Carrara, A., Clement, R., Dellwik, E., Elbers, J., Eugster, W., Fuhrer, J., Granier, A., Grünwald, T., Heinesch, B., Janssens, I.A., Knohl, A., Koeble, R., Laurila, T., Longdoz, B., Manca, G., Marek, M., Markkanen, T., Mateus, J., Matteucci, G., Mauder, M., Migliavacca, M., Minerbi, S., Moncrieff, J., Montagnani, L., Moors, E., Ourcival, J.-M., Papale, D., Pereira, J., Pilegaard, K., Pita, G., Rambal, S., Rebmann, C., Rodrigues, A., Rotenberg, E., Sanz, M.J., Sedlak, P., Seufert, G., Siebicke, L., Soussana, J.F., Valentini, R., Vesala, T., Verbeeck, H., Yakir, D., 2008. Quality control of CarboEurope flux data – Part 1: coupling footprint analysis with flux data quality assessment to evaluate sites in forest ecosystems. *Biogeosciences* 5, 433–450.
- Graf, A., Schüttmeier, D., Geiß, H., Knaps, A., Möllmann-Coers, M., Schween, J.H., Kollet, S., Neining, B., Herbst, M., Vereecken, H., 2010. Boundedness of turbulent temperature probability distributions, and their relation to the vertical profile in the convective boundary layer. *Bound.-Layer Meteorol.* 134, 459–486. doi:10.1007/s10546-009-r9444-9.
- Grünwald, T., Bernhofer, Ch., 2007. A decade of carbon, water and energy flux measurements of an old spruce forest at the Anchor Station Tharandt. *Tellus* 59B, 387–396.
- Grunzweig, J.M., Lin, T., Rotenberg, E., Schwartz, A., Yakir, D., 2003. Carbon sequestration in arid-land forest. *Global Change Biol.* 9 (5), 791–799.
- Haslwanter, A., Hammerle, A., Wohlfahrt, G., 2009. Open-path vs. closed-path eddy covariance measurements of the net ecosystem carbon dioxide and water vapour exchange: a long-term perspective. *Agric. Forest Meteorol.* 149, 291–302. doi:10.1016/j.agrformet.2008.08.011.
- Hatakka, J., Aalto, T., Aaltonen, V., Aurela, M., Hakola, H., Komppula, M., Laurila, T., Lihavainen, H., Paatero, J., Salminen, K., Viisanen, Y., 2003. Overview of the atmospheric research activities and results at Pallas GAW station. *Boreal Environ. Res.* 8, 365–383.
- Heusinkveld, B.G., Jacobs, A.F.G., Holtslag, A.A.M., Berkowicz, S.M., 2004. Surface energy balance closure in an arid region: role of soil heat flux. *Agricu. Forest Meteorol.* 122, 21–37.
- Hibbard, K.A., Law, B.E., Reichstein, M., Sulzman, J., 2005. An analysis of soil respiration across northern hemisphere temperate ecosystems. *Biogeochemistry* 73, 29–70.
- Huang, J., Lee, X., Patton, E.G., 2009. Dissimilarity of scalar transport in the convective boundary layer in inhomogeneous landscapes. *Bound.-Layer Meteorol.* 130, 327–345. doi:10.1007/s10546-009-r9356-8.
- Inagaki, A., Letzel, M.O., Raasch, S., Kanda, M., 2006. Impact of surface heterogeneity on energy imbalance: a study using LES. *J. Meteor. Soc. Japan* 84 (1), 187–198.
- Jaeger, E.B., Stöckli, R., Seneviratne, S.I., 2009. Analysis of planetary boundary layer fluxes and land-atmosphere coupling in the Regional Climate Model CLM. *J. Geophys. Res. -Atmos.* 114, D17106.
- Jarvis, P.G., Massheder, J.M., Hale, S.E., Moncrieff, J.B., Rayment, M., Scott, S.L., 1997. Seasonal variation of carbon dioxide, water vapor, and energy exchanges of a boreal black spruce forest. *J. Geophys. Res.* 102, 953–966. doi:10.1029/97JD01176.
- Kanda, M., Inagaki, A., Letzel, M.O., Raasch, S., Watanabe, T., 2004. LES study of the energy imbalance problem with eddy covariance fluxes. *Bound.-Layer Meteorol.* 110, 381–404.
- Koster, R.D., Dirmeyer, P.A., Guo, Z.C., Bonan, G., Chan, E., Cox, P., Gordon, C.T., Kanae, S., Kowalczyk, E., Lawrence, D., Liu, P., Lu, C.H., Malyshev, S., McAvaney, B., Mitchell, K., Mocko, D., Oki, T., Oleson, K., Pitman, A., Sud, Y.C., Taylor, C.M., Verseghy, D., Vasic, R., Xue, Y.K., Yamada, T., 2004. Regions of strong coupling between soil moisture and precipitation. *Science* 305, 1138–1140.
- Kutsch, W.L., Persson, T., Schrupp, M., Moyano, F.E., Mund, M., Andersson, S., Schulze E.-D., 2010. Heterotrophic soil respiration and soil carbon dynamics in

- the deciduous Hainich forest obtained by three approaches. *Biogeochemistry*. doi:10.1007/s10533-010-r9414-9.
- Marcolla, A., Pitacco, A., Cescatti, A., 2003. Canopy architecture and turbulence structure in a coniferous forest. *Bound.-Layer Meteor.* 108, 39–59.
- Mauder, M., Jegede, O.O., Okogbue, E.C., Wimmer, F., Foken, T., 2007. Surface energy flux measurements at a tropical site in West-Africa during the transition from dry to wet season. *Theor. Appl. Climatol.* 89, 171–183.
- Mauder, M., Desjardins, R.L., Pattey, E., Gao, Z., van Haarlem, R., 2008. Measurement of the sensible eddy heat flux based on spatial averaging of continuous ground-based observations. *Bound.-Layer Meteor.* 128, 151–172.
- Meyers, T.P., Hollinger, S.E., 2004. An assessment of storage terms in the surface energy balance of maize and soybean. *Agricu. Forest Meteor.* 125, 105–115.
- Migliavacca, M., Meroni, M., Manca, G., Matteucci, G., Montagnani, L., Grassi, G., Zenone, T., Teobaldelli, M., Godec, I., Colombo, R., Seufert, G., 2009. Seasonal and interannual patterns of carbon and water fluxes of a poplar plantation under peculiar eco-climatic conditions. *Agric. Forest Meteor.* 149, 1460–1474.
- Milyukova, I.M., Kolle, O., Varlagin, A.V., Vygodskaya, N.N., Schulze, E.D.F., Lloyd, J., 2002. Carbon balance of a southern taiga spruce stand in European Russia. *Tellus Ser. B* 54, 429–442.
- Moureaux, C., Debacq, A., Bodson, B., Heinesch, B., Aubinet, M., 2006. Annual net ecosystem carbon exchange by a sugar beet crop. *Agric. Forest Meteor.* 139, 25–39.
- Rebmann, C., Zeri, M., Lasslop, G., Mund, M., Kolle, O., Schulze, E.-D., Feigenwinter, Ch., 2010. Treatment and assessment of the CO₂-exchange at a complex forest site in Thuringia, Germany. *Agric. Forest Meteor.* 150, 684–691. doi:10.1016/j.agrformet.2009.11.001.
- Richardson, A.D., Hollinger, D.Y., Burba, G.G., Davis, K.J., Flanagan, L.B., Katul, G.G., Munger, J.W., Ricciuto, D.M., Stoy, P.C., Verma, S.B., Wofsy, S.C., 2006. A multi-site analysis of random error in tower-based measurements of carbon and energy fluxes. *Agric. Forest Meteor.* 136, 1–18.
- Reichstein, M., Tenhunen, J.D., Rouspard, O., Ourcival, J.M., Rambal, S., Miglietta, F., Peressotti, A., Pecchiari, M., Tirone, G., Valentini, R., 2002. Severe drought effects on ecosystem CO₂ and H₂O fluxes at three Mediterranean evergreen sites: revision of current hypotheses? *Global Change Biol.* 8, 999–1017.
- Reichstein, M., Rey, A., Freibauer, A., Tenhunen, J., Valentini, R., Banza, J., Casals, P., Cheng, Y.F., Grunzweig, J.M., Irvine, J., Joffre, R., Law, B.E., Loustau, D., Miglietta, F., Oechel, W., Ourcival, J.M., Pereira, J.S., Peressotti, A., Ponti, F., Qi, Y., Rambal, S., Rayment, M., Rom, J., 2003. Modeling temporal and large-scale spatial variability of soil respiration from soil water availability, temperature and vegetation productivity indices. *Global Biogeochem. Cycles* 17 (4), 1104. doi:10.1029/2003GB002035.
- Reichstein, M., Falge, E., Baldocchi, D., Papale, D., Aubinet, M., Berbigier, P., Bernhofer, C., Buchmann, N., Gilmanov, T., Granier, A., Grunwald, T., Havrankova, K., Ilvesniemi, H., Janous, D., Knohl, A., Laurila, T., Lohila, A., Loustau, D., Matteucci, G., Meyers, T., Miglietta, F., Ourcival, J.-M., Pumpanen, J., Rambal, S., Rotenberg, E., Sanz, M., Tenhunen, J., Seufert, G., Vaccari, F., Vesala, T., Yakir, D., Valentini, R., 2005. On the separation of net ecosystem exchange into assimilation and ecosystem respiration: review and improved algorithm. *Global Change Biol.* 11 (9), 1424–1439.
- Richardson, A.D., Mahecha, M.D., Falge, E., Kattge, J., Moffat, A.M., Papale, D., Reichstein, M., Stauch, V.J., Braswell, B.H., Churkina, G., Kruij, B., Hollinger, D.Y., 2008. Statistical properties of random CO₂ flux measurement uncertainty inferred from model residuals. *Agricu. Forest Meteor.* 148, 38–50.
- Schmid, H.P., Su, H.B., Vogel, C.S., Curtis, P.S., 2003. Ecosystem-atmosphere exchange of carbon dioxide over a mixed hardwood forest in northern lower Michigan. *J. Geophys. Res.* 108, (D14), 4417. doi:10.1029/2002JD003011.
- Seneviratne, S.I., Lüthi, D., Litschi, M., Schär, C., 2006. Land-atmosphere coupling and climate change in Europe. *Nature* 443, 205–209.
- Staudt, K., Foken, T., 2007. Documentation of reference data for the experimental areas of the Bayreuth Center for Ecology and Environmental Research (BayCEER) at the Waldstein site. *Arb. Ergebnisse* No. 35, Dep. Micrometeorol., University of Bayreuth.
- Stöckli, R., Lawrence, D.M., Niu, G.-Y., Oleson, K.W., Thornton, P.E., Yang, Z.-L., Bonan, G.B., Denning, A.S., Running, S.W., 2008. Use of FLUXNET in the community land model development. *J. Geophys. Res.* 113, G01025. doi:10.1029/2007JG000562.
- Tanaka, H., Hiyama, T., Kobayashi, N., Yabuki, H., Ishii, Y., Desyatkin, R.V., Maximov, T.C., Ohta, T., 2008. Energy balance and its closure over a young larch forest in eastern Siberia. *Agricu. Forest Meteor.* 148 (12), 1954–1967. doi:10.1016/j.agrformet.2008.05.006.
- Twine, T.E., Kustas, W.P., Norman, J.M., Cook, D.R., Houser, P.R., Meyers, T.P., Prueger, J.H., Starks, P.J., Wesely, M.L., 2000. Correcting eddy-covariance flux underestimates over a grassland. *Agric. Forest Meteor.* 103, 279–300.
- Valentini, R., Matteucci, G., Dolman, A.J., Schulze, E.D., Rebmann, C., Moors, E.J., Granier, A., Gross, P., Jensen, N.O., Pilegaard, K., Lindroth, A., Grelle, A., Bernhofer, C., Grunwald, T., Aubinet, M., Ceulemans, R., Kowalski, A.S., Vesala, T., Rannik, U., Berbigier, P., Loustau, D., Guomundsson, J., Thorgeirsson, H., Ibrom, A., Morgenstern, K., Clement, R., Moncrieff, J., Montagnani, L., Minerbi, S., Jarvis, P.G., 2000. Respiration as the main determinant of carbon balance in European forests. *Nature* 404, 861–865.
- Vanderborgh, J., Graf, A., Steenpass, C., Scharnagl, B., Prolingheuer, N., Herbst, M., Hendricks Franssen, H.J., Vereecken, H., 2010. Effect of within-field soil type variability on the variability of bare soil evaporation: comparison of eddy covariance measurements with potential and actual evaporation calculations. *Vadose Zone J.*
- Wilson, K., Goldstein, A., Falge, E., Aubinet, M., Baldocchi, D., Berbigier, P., Bernhofer, C., Ceulemans, R., Dolman, H., Field, C., Grelle, A., Ibrom, A., Law, B.E., Kowalski, A., Meyers, T., Moncrieff, J., Monson, R., Oechel, W., Tenhunen, J., Valentini, R., Verma, S., 2002. Energy balance closure at FLUXNET sites. *Agric. Forest Meteor.* 113, 223–243.